Tan *et al. Financial Innovation* (2022) 8:64
https://doi.org/10.1186/s40854-022-00369-y

Financial Innovation

RESEARCH Open Access

DeepPricing: pricing convertible bonds based on financial time-series generative adversarial networks

Xiaoyu Tan[1,2*], Zili Zhang[2], Xuejun Zhao[2] and Shuyi Wang[3*]

*Correspondence:
tanxy01@jsfund.cn;
shuyiw@zju.edu.cn

[2] Harvest Fund Management, Beijing 100020, China
[3] Department of Mathematics, Zhejiang University, Hangzhou 310027, China
Full list of author information is available at the end of the article

Abstract

Convertible bonds are an important segment of the corporate bond market, however, as hybrid instruments, convertible bonds are difficult to value because they depend on variables related to the underlying stock, the fixed-income part, and the interaction between these components. Besides, embedded options, such as conversion, call, and put provisions are often restricted to certain periods, may vary over time, and are subject to additional path-dependent features of the state variables. Moreover, the most challenging problem in convertible bond valuation is the underlying stock return process modeling as it retains various complex statistical properties. In this paper, we propose *DeepPricing*, a novel data-driven convertible bonds pricing model, which is inspired by the recent success of generative adversarial networks (GAN), to address the above challenges. The method introduces a new financial time-series generative adversarial networks (*FinGAN*), which is able to reproduce risk-neutral stock return process that retains the unique statistical properties such as the fat-tailed distributions, the long-range dependence, and the asymmetry structure etc., and then transit to its risk-neutral distribution. Thus it is more flexible and accurate to capture the dynamics of the underlying stock return process and keep the rich set of real-world convertible bond specifications compared with previous model-driven models. The experiments on the Chinese convertible bond market demonstrate the effectiveness of *DeepPricing* model. Compared with the convertible bond market prices, our model has a better convertible bonds pricing performance than both model-driven models, i.e. Black-Scholes, the constant elasticity of variance, GARCH, and the state-of-the-art GAN-based models, i.e. FinGAN-MLP, FinGAN-LSTM. Moreover, our model has a better fitting capacity for higher-volatility convertible bonds and the overall convertible bond market implied volatility smirk, especially for equity-liked convertible bonds, convertible bonds trading in the bull market, and out-of-the-money convertible bonds. Furthermore, the *Long-Short* and *Long-Only* investment strategies based on our model earn a significant annualized return with 41.16% and 31.06%, respectively, for the equally-weighted portfolio during the sample period.

Keywords: Convertible bonds, Generative adversarial network, Time-series simulation, Pricing, Investment strategy, Artificial intelligence

JEL Classification: G1, G12, C5, C6, C63

Introductions

As an important part of the corporate bond market, convertible bonds with both equity- and debt-like properties have grown in popularity in the financial market. However, compared with the nearly 150-years industry practice of convertible bonds, the development of convertible bond pricing theory lags behind. This is not surprising as convertible bonds cannot simply be considered as a combination of equity and bonds but various terms of realistic convertible bonds, such as the possibility of early conversion, the callability by the issuer, and the putability by the holder, making it difficult to value.

Traditional theoretical research on convertible bond pricing can be roughly divided into three categories. The first pricing approach implies finding a closed-form solution to the valuation equation. It was initiated by Ingersoll (1977) who applies the contingent claims approach to the valuation of convertible bonds. Lewis (1991) develops a closed-form solution for convertible bonds that accounts for more complex capital structures. This kind of valuation model was established with the option pricing models of Black and Scholes (1973) and Merton (1973, 1974) and value the convertible bonds based on their firm value or stock value (McConnell and Schwartz 1986) as the underlying state variable. Later, Nyborg (1996) obtained a closed-form solution for most basic convertible bonds, where conversion is only allowed at maturity, while Zhu (2006) presented an analytical solution for the convertible bonds, which can be converted at any time on or before maturity. Although fast in computation, closed-form solutions are not suitable for empirical studies because they fail to account for several real-world specifications. Especially, dividends and coupon payments are often modeled continuously rather than discretely, early-exercise features are omitted, and path-dependent features are excluded. The second pricing approach values convertible bonds numerically, using lattice-based methods. In general, among lattice-based methods, there are finite difference methods (e.g. Brennan and Schwartz 1977; Tsiveriotis and Fernandes 1998; Takahashi et al. 2001; Ayache et al. 2003; Zhu et al. 2018; Lin and Zhu 2020), finite element method (e.g. Barone-Adesi et al. 2003), tree model (e.g. Hung and Wang 2002; Chambers and Lu 2007; Yagi and Sawaki 2010; Ma et al. 2020); some of the lattice-based models provide sophisticated pricing and calibration solutions. Besides, in the face of practical problems related to real convertible-bond specifications and limited data availability, the proposed approaches turn out to be practicable only in very few cases. The third class of convertible bond pricing method uses least-squares Monte Carlo (LSM) simulation (e.g. Buchan 1997; Ammann et al. 2008; Fan et al. 2017; Batten et al. 2018). LSM proposed by Longstaff and Schwartz (2001) is suitable for modeling discrete coupon and dividend payments, including dynamics of the underlying state variables, taking into account path-dependent option features, and overcoming many of the drawbacks of lattice-based methods. The most important input in LSM is the assumption and generation of underlying stock return process, such as the Black-Scholes (BS) model, the constant elasticity of variance (CEV) model, or the GARCH model. However, building on the limitation of explicit mathematical formulations, the models are difficult to recover all unique statistial properties such as the leverage effects, the coarse-fine volatility correlation, and the gain/loss asymmetry of financial time-series (Malmsten and Teräsvirta 2010; Takahashi et al. 2019; Dogariu et al. 2022).

Considering the difficulties of the existing pricing approaches, it is desirable to develop an alternative data-driven path simulator that has a high reproducibility of stylized facts and can be built without many assumptions. Deep learning, especially generative adversarial networks (GAN), proposed by Goodfellow et al. (2014), which bears the potential of being able to model complicated statistical (perhaps unknown) dynamic may provide such a solution. GAN-based methods have already shown spectacular ability in the generation of data including realistic image (Radford et al. 2015; Karras et al. 2021), audio (Donahue et al. 2018), natural language text (Zhang et al. 2016; Garbacea et al. 2019) and have expanded to sequence generation, such as physics (Farimani et al. 2017; Li et al. (2019), music (Yang et al. 2017; Gan et al. 2020), medical time-series (Esteban et al. 2017; Sun et al. 2020), DNA sequences (Killoran et al. 2017; Gupta and Zou 2019) and financial time-series (Takahashi et al. 2019; Wiese et al. 2020). Moreover, the GAN architectures also show the benefits in the financial time-series representation learning, such as stock price prediction (Zhang et al. 2019; Dogariu et al. 2022), disentangle market behaviors from the price movement of stocks (Hadad et al. 2018), and systematic trading strategies (Koshiyama et al. 2021). As it remains the problem of transiting the real (observable) financial time series to its risk-neutral distribution, the GAN-based approaches have not been successfully applied to classical LSM to generate stock return process and solve the problem of derivatives pricing (Wiese et al. 2020).

In this paper, we propose *DeepPricing*, a novel financial time-series generative adversarial networks (*FinGAN*) based convertible bonds pricing model in the framework of LSM to address the challenges above. Our primary contributions are twofold. First, we extend the literature on derivatives pricing, especially convertible bonds pricing, by showing that GAN-based approaches can be successfully applied to the framework of LSM. The model is more flexible and accurate to capture the temporal structures of financial time-series so as to generate the major stylized facts of the underlying stock returns, including the linear unpredictability, the fat-tailed distribution, the volatility clustering, the leverage effects, the coarse-fine volatility correlation, and the gain/loss asymmetry, and then transit to its risk-neutral distribution. Second, a new mechanism, *FinGAN*, is explicitly constructed to generate stochastic underlying stock return process and transit to its risk-neutral distribution. We introduce an encoder network to provide a mapping between feature and neutral space, thereby separating the features of volatility and drift in the adversarial learning space. This capitalizes on the fact that during the risk-neutral measure transformation process, the volatility features have been retained while the drift features have been changed to the risk-free rate (Shreve 2004). Moreover, the supervised loss is minimized by jointly training both the embedding and generator networks, so that the neutral space not only serves to promote parameter efficiency but is also specifically conditioned to facilitate the generator in learning volatility features.

Empirically, we evaluate the capacity of the *DeepPricing* in the Chinese convertible bonds market in two steps. First, the statistical properties of the generated time-series from *FinGAN* and other baseline generators are analyzed and compared with the real financial time-series, and then the convertible bond pricing performances test is conducted across the *DeepPricing* and other baseline convertible bond valuation models. Several important conclusions can be drawn from the empirical results. First, the *FinGAN* model achieves consistent improvements over both traditional and state-of-the-art

benchmarks in generating major statistical properties of stock returns, including the linear unpredictability, the fat-tailed distributions, the volatility clustering, the leverage effects, the coarse-fine volatility correlation, and the gain/loss asymmetry. Second, compared with real convertible bonds market prices, the *DeepPricing* model has a better convertible bonds pricing performance than both model-driven models, i.e. BS, CEV ($\beta = 1$), GARCH (1,1) and data-driven models, i.e. FinGAN-MLP, FinGAN-LSTM. Third, we have broken down convertible bonds according to their equity component levels, market states, and moneyness levels to investigate the ability of the models to fit the structure of the convertible bonds market. The empirical results show that the *DeepPricing* model has a better fitting capacity for the equity-liked, trading in the bull market and out-of-the-money convertible bonds. Generally speaking, the results indicate that due to the *FinGAN* generator's higher reproducibility of stylized facts, the *DeepPricing* model is more flexible and consistent to capture the volatility and high-dimensional features of the underlying stock process thus outperforming other models in fitting higher volatility convertible bonds and the overall convertible bond market implied volatility smirk. The results also demonstrate the simulation of the dynamic process of the underlying stock return has a significant effect on the efficiency of convertible bond pricing, which is consistent with the empirical conclusion of Batten et al. (2018) in U.S. convertible bond market.

Furthermore, we analyze the factors affecting the pricing of Chinese convertible bonds. Empirical results show that convertible bonds which are higher-liquidity, riskier (longer time to maturity, lower quality credit rating, higher volatility), equity-liked, trading in the bull market and out-of-the-money tend to be more likely to be mispriced. The results are consistent with the convertible bond pricing performance, and further illustrate the importance of accurately characterizing the volatility and high-dimensional features for the pricing of convertible bonds. Besides, considering the Chinese convertible bond market is a weak efficient market, thus, we propose investment strategies based on the *DeepPricing* model. Both *Long-Short Strategy* and *Long-Only Strategy* earn a significant annualized return with 41.16% and 31.06%, respectively, for the equally-weighted portfolio during January 01, 2018 to June 30, 2021, respectively.

The rest of the paper is organized as follows. "Preliminaries" section gives the basic terms and payoff structure of convertible bonds. "The DeepPricing model" section develops the methods used in the paper. "Data and experiment" section provides the descriptive statistics of the Chinese convertible bond market and empirical results across the *DeepPricing* model and the baseline models. "Investment strategies" section introduces the investment strategies based on the *DeepPricing* model. "Conclusion" section concludes.

Preliminaries

Convertible bonds are corporate debt securities that give the holder the right to forego future coupon and/or principal payments and receive (i.e., convert to) a prespecified number of shares of common stock instead. In principal, a convertible bond is hybrid security consisting of a straight bond and a call on the underlying equity, but various terms of realistic convertible bonds make it impossible to decouple the stock option from the bond part. Furthermore, due to the existence of these special terms, the payoff

structure of convertible bonds is really complicated. Thus, before introducing the pricing model, we first give the basic terms of convertible bonds in "Basic terms" section, and then present the payoff structure of convertible bonds in "Payoff structure" section.

Basic terms

Generally speaking, taking the Chinese convertible bonds as an example, convertible bonds mainly have the following four types option terms:

Conversion terms: Investors can execute conversion rights within a certain period of time ($t \in \Omega_{\text{conv}}$). In case of conversion, the investor receives $n_t S_t$, where S_t is the underlying stock price at time t, $n_t = B_t/K_t$ is the conversion ratio (the number of stocks available per unit of bonds exchanged), K_t is the conversion price, and B_t is the face value of the convertible bond.

Conditional redemption terms: This term allows the issuer to demand premature redemption in exchange for the redemption price C_t applicable at time t under certain conditions (usually, if S_t is not less than 130% of the $n_t S_t$ for at least 15 trading days in any 30 consecutive trading days and $t \in \Omega_{\text{call}}$). The issuer is obliged to announce his/her intention to redemption a certain period in advance, referred to as the call notice period. If the convertible bond is premature redemption, the investor may want to exercise his/her conversion option at any time during the call notice period to receive the conversion value instead of the redemption price.

Repurchase terms: This term entitles the investor to force the issuing firm to prematurely repurchase the convertible bonds for a certain predefined price P_t under certain conditions (usually, if S_t is lower than 70% of the $n_t S_t$ for 30 consecutive trading days and $t \in \Omega_{\text{put}}$).

Conversion price revision terms: This term entitles the company's board of directors the right to propose a downward revision plan for the conversion price from K_t to K_t^* to avoid trigger repurchase under certain conditions (usually, if S_t is lower than 85% of the $n_t S_t$ for at least 10 trading days in any 20 consecutive trading days and $t \in \Omega_{\text{conv}}$).

Payoff structure

The payoff of a convertible bond depends on whether and when the investor and the issuer decide to exercise their options and trigger the termination of the convertible bond. Let τ^* be the optimal stopping time, i.e. the time at which it is optimal for either the issuer or the investor to terminate the convertible bond.

The resulting action may either be conditional redemption, forced conversion, voluntary conversion, repurchase, regular redemption when the bond matures or default. Formally, the optimal stopping time of the convertible bond is defined as $\tau* = \min\{t : \psi(X_t, t) \neq 0\}$, where $\psi(X_t, t)$ is the payoff resulting from the convertible bond in state X_t at time t, given the optimal option-exercise behavior of both investor and issuer.

The alternatives presented in Table 1 stand for all events that will cause the convertible bond to be terminated and reflect boundary conditions that impede arbitrage opportunities. The optimal exercise decision critically depends on the value of continuation V_t, i.e. the conditional expected value of the convertible bond if it is not exercised immediately.

Table 1 Payoff structure of convertible bonds

Payoff	Boundary condition	Time restriction	State
C_t	$V_t > C_t$ and $C_t > n_t S_t$	For $t \in \Omega_{\text{conv}} \cap \Omega_{\text{call}}$	Conditional redemption
$n_t S_t$	$V_t > K_t$ and $n_t S_t > K_t$	For $t \in \Omega_{\text{conv}}$	Forced conversion
$n_t S_t$	$n_t S_t > C_t$ and $P_t < n_t S_t$	For $t \in \Omega_{\text{conv}}$	Voluntary conversion
0	$V_t < C_t$; $V_t > n_t S_t$ and $V_t < P_t$	For $t \in \Omega_{\text{conv}}$	Continuation
P_t	$P_t > V_t$ and $n_t S_t < P_t$	For $t \in \Omega_{\text{put}}$	Repurchase
κB	$n_t S_t < \kappa B$	For $t = T \in \Omega_{\text{put}}$	Redemption at maturity
$\theta \kappa B$	$V_t < \theta \kappa B$	For $t \in [0, T]$	Default

Table 1 summarizes the payoff structure of convertible bonds at maturity and prior to maturity subject to the boundary conditions. *Time Restriction* indicates the set of times in which conversion can be exercised, as stated in the issuance contract. And *State* lists the optimal strategies to be undertaken when the boundary conditions are met. Where V_t is the conditional expected value of continuation, C_t is the redemption price when the *Conditional Redemption Terms* is triggered, $n_t S_t$ is the conversion value, P_t is the repurchase price when the *Repurchase Terms* is triggered, κB is a pre-specified amount when convertible bond is redeemed at the time of maturity, B is the face value of the convertible bond and κ is the final redemption ratio of the face value, θ is the recovery rate when the convertible bond defaults

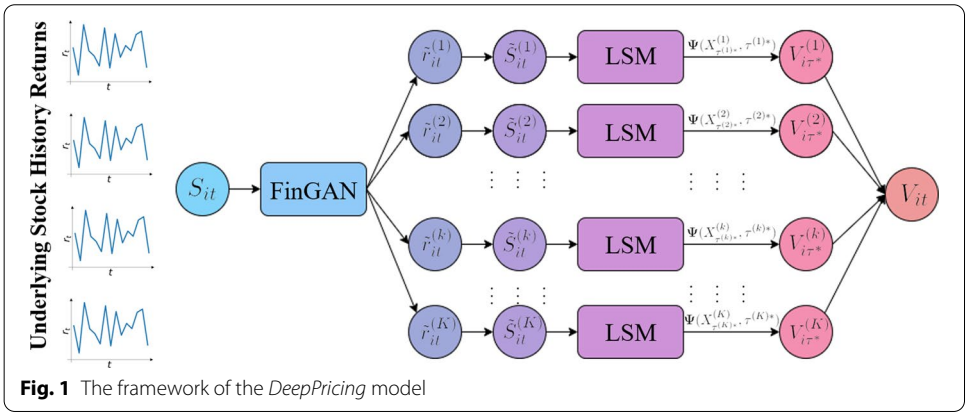

Fig. 1 The framework of the *DeepPricing* model

In addition to the payoff at the time of termination, the investor receives all coupon payments that occurred prior to the time of termination from his/her convertible bond investment. Formally, the function $\Psi(X_{\tau^*}, \tau^*)$ represents the total payoff from a convertible bond in state X_{τ^*} and at time τ^*:

$$\Psi(X_{\tau^*}, \tau^*) = \psi(X_{\tau^*}, \tau^*) + \eta(\tau^*) \tag{1}$$

where $\psi(X_{\tau^*}, \tau^*)$ is the payoff from the convertible bond at the optimal stopping time τ^* and $\eta(\tau^*)$ is the present value at time τ^* of all coupon payments accumulated during the existence of the bond, i.e. before τ^*.

The DeepPricing model

In this section, we propose a generative adversarial networks (GAN) based model called *DeepPricing* to price convertible bonds. As shown in Fig. 1, the *DeepPricing* model mainly contains two components. The first component is a novel Financial time-series Generative Adversarial Networks (*FinGAN*). For each convertible bond *i*, we use the

FinGAN model to generate several underlying stock return processes $r_i^{(k)}$, and then transit them to their risk-neutral distribution $\tilde{r}_i^{(k)}$. The second component is the least-squares Monte Carlo (LSM) approach, which was proposed by Longstaff and Schwartz (2001). For each generate and transit underlying stock path $\tilde{S}_i^{(k)}$, we use the least-squares to estimate the conditional expected payoff $\Psi(X^{(k)}_{\tau^{(k)*}}, \tau^{(k)*})$ to the optimal exercise strategy of the investor and the issuer from continuation. Then, the price of convertible bond i at time t in path k can be obtained by discounting all future cash flows under risk-neutral measure. Given a risk-neutral probability space $(\Omega, \mathcal{F}, \mathbb{Q})$ and information filtration $\mathcal{F}_t$, the value of convertible bond i is given by:

$$V_{it}^{(k)} = E^{\mathbb{Q}}\left[e^{-\sum_{s=t}^{\tau^{(k)*}-1} r(X_s^{(k)},s)} \Psi(X^{(k)}_{\tau^{(k)*}}, \tau^{(k)*}) | \mathcal{F}_t\right] \tag{2}$$

where $V_{it}^{(k)}$ is the value of the convertible bond i at time t in path k, $\tau^{(k)*}$ is the optimal stopping time taking values in the finite set $\{0, 1, \cdots, T\}$, and the function $\Psi(X^{(k)}_{\tau^{(k)*}}, \tau^{(k)*})$ represents the total payoff from a convertible bond i in path k defined in Eq. 1. The expectation $r(X_s^{(k)}, s)$ is the interest rate of the time interval $[s, s+1]$ in state X_s, and is also applicable for discounting cash flows from time $s+1$ to s. Finally, we average the value of convertible bond along each path ($V_{it}^{(k)}$) as the final value of convertible bond i (V_{it}).

Stock dynamic simulation: *FinGAN*

The most important input in convertible bonds valuation is the assumption of the underlying stock process, especially the volatility of the underlying stock returns under risk-neutral probability space (Ammann et al. 2008, Batten et al. 2018). However, modeling financial time-series is a challenging task as it retains various complex statistical properties such as the linear unpredictability, the fat-tailed distributions, the volatility clustering, the leverage effects, the coarse-fine volatility correlation, and the gain/loss asymmetry, it is desirable to develop an alternative approach that has a high reproducibility of stylized facts and can be built without a number of assumptions. In this section, we propose *FinGAN*, a novel deep neural networks based approach which can capture the temporal structures of financial time-series so as to generate major stylized facts of stock process mentioned above, and then transform them into risk-neutral probability space. We first give the network framework of *FinGAN* model in "Network architecture" section. Furthermore, we introduce the derivation process from *FinGAN* to the stock price process in "Theoretical basis" section to strengthen the theoretical interpretation of our model.

Network architecture

FinGAN consists of four network components: an encoder function, decoder function, Risk-Neutral Networks (RiNN) generator, and discriminator. The key insight is that the auto-encoding components (first two) are trained jointly with the risk-neutral adversarial components (latter two), such that *FinGAN* simultaneously learns to *encode* features, *generate* and *transfer* representations, and *iterate* across time. The encoder-decoder network provides the latent neutral space, the adversarial network operates within this space, and the latent dynamics of both neutral and synthetic data are synchronized

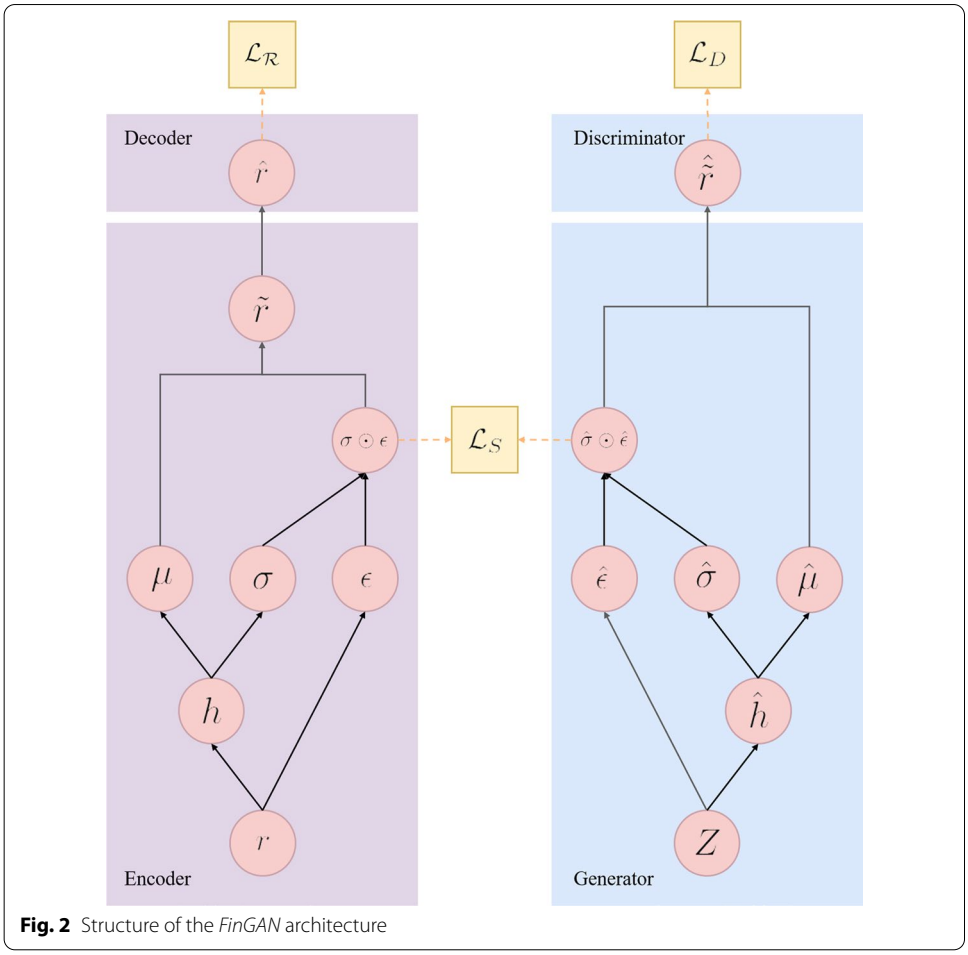

Fig. 2 Structure of the *FinGAN* architecture

through a supervised loss. The detailed architecture is shown in Fig. 2 and we describe each in turn[1].

Encoder and decoder functions: The encoder and decoder functions provide mappings between the real sequence space and the latent risk-neutral sequence space, allowing the adversarial generative network to transfer the real stock return process to its risk-neutral distribution. The encoder function extracts the volatility (σ_t), drift (μ_t), and innovation (ϵ_t) terms from the real log-return series, and then we use Eq. 20 to reconstruct the risk-neutral series ($\tilde{r}_t$). Specifically, σ_t and μ_t at time t are generated by $r_{(t-T):(t-1)}$ through the embedding network en_h for the volatility and drift features, while ϵ_t is generated by r_t through the embedding network en_ϵ for the innovation features. As shown in the Fig. 3, we choose temporal convolutional networks (TCN) as the basic network compositions of the encoder[2], which is particularly suited for

[1] Notice that throughout this section, $n, m \in \mathbb{N}$. $r, \tilde{r}, \hat{r}$ and $\hat{\tilde{r}}$ are $\mathbb{R}^n$-valued random variables, Z is $\mathbb{R}^m$-valued random variable.

[2] Empirical results suggest that TCN is able to capture long-range dependencies in sequences more effectively than well-known recurrent architectures (Goodfellow et al. 2016) such as the gated recurrent unit (GRU, Chung et al. 2014) or the long short-term memory (LSTM, Zhang et al. 2019). One of the main advantages of TCN is the absence of exponentially vanishing and exploding gradients through time (Pascanu et al. 2013), which is one of the main issues why recurrent neural networks (RNN) are difficult to optimize. Although LSTM addresses this issue by using gated activations, empirical studies show that TCN performs better on supervised learning benchmarks (Bai et al. 2018).

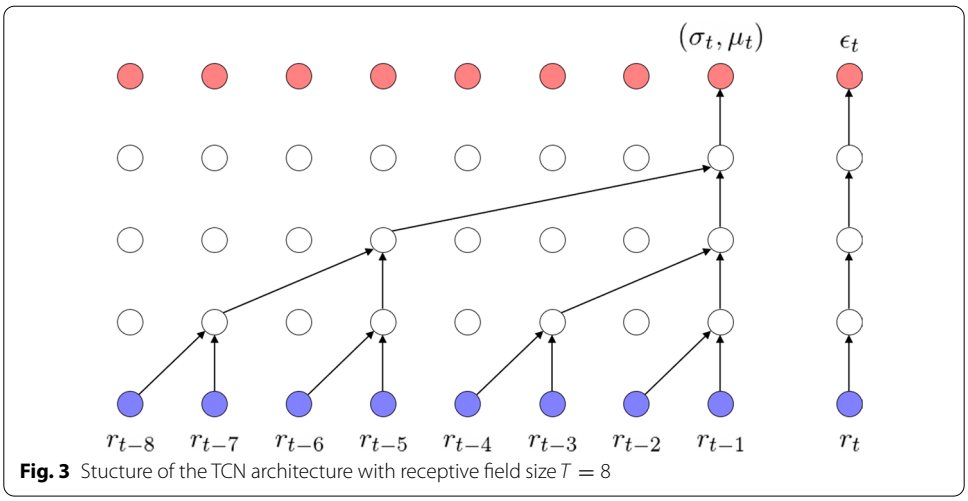

Fig. 3 Stucture of the TCN architecture with receptive field size $T = 8$

modeling long-range dependencies, allows for parallelization, and guarantees stationarity. The definition of the encoder is given by Def. 1,

Definition 1 *(Encoder)* Let input $r_{in,t}$ be $\mathbb{R}^n$-valued, $en_h : \mathbb{R}^{n\times \mathrm{T}} \times \Theta_{en}^{(h)} \to \mathbb{R}^{2n}$ be an encoder network with receptive field size T and $en_\epsilon : \mathbb{R}^n \times \Theta_{en}^{(\epsilon)} \to \mathbb{R}^n$ be a network. Furthermore, $\alpha \in \Theta_{en}^{(h)}$ and $\beta \in \Theta_{en}^{(\epsilon)}$ denote some parameters. The log-return neural process $\tilde{\mathrm{r}}$ in feature spaces is defined by:

$$\begin{aligned} \tilde{\mathrm{r}} : \Omega \times \mathbb{R}^{n\times T} \times \Theta_{en}^{(h)} \times \Theta_{en}^{(\epsilon)} &\to \mathbb{R}^n \\ (\omega, t, \alpha, \beta) &\mapsto [\sigma_{t,\alpha} \odot \epsilon_{t,\beta} + \mu_{t,\alpha}](\omega) \end{aligned} \tag{3}$$

where $\odot$ denotes the Hadamard product and

$$\begin{aligned} h_t &:= en_h(\mathrm{r}_{\mathrm{in},(t-\mathrm{T}):(t-1)}), \\ \sigma_{t,\alpha} &:= |h_{t,1:n}|, \\ \mu_{t,\alpha} &:= h_{t,n+1:2n}, \\ \epsilon_{t,\beta} &:= en_\epsilon(\mathrm{r}_{\mathrm{in},(t)}). \end{aligned} \tag{4}$$

Notably, the encoder network separate the log-return process into volatility and drift features and transit them to risk-neutral distribution. The neural process $\sigma_{t,\alpha} := (\sigma_{t,\alpha})_{t\in\mathbb{R}}$, $\mu_{t,\alpha} := (\mu_{t,\alpha})_{t\in\mathbb{R}}$, $\mathrm{r}_{f(t,\alpha)} := (\mathrm{r}_{f(t,\alpha)})_{t\in\mathbb{R}}$ and $\epsilon_{t,\beta} := (\epsilon_{t,\beta})_{t\in\mathbb{R}}$ and are called volatility, drift, risk-neutral and innovation neural process, respectively.

In the opposite direction, the decoder function transforms the risk-neutral series $(\tilde{r}_t)$ back to the estimated original market data $(\hat{r}_t)$. Notice that, just as the long-range dependencies of the encoder is emphasized before, the network of decoder needs to satisfy such properties as well. Thus, we also implement decoder by TCNs. The definition of the decoder is given by Def. 2,

Definition 2 *(Decoder)* Let $l \in \mathbb{N}$, and $de : \mathbb{R}^{n\times l} \times \Theta_{de} \to \mathbb{R}^{n\times l}$ be a network with parameter space Θ_{de}. The time-series $\hat{r}$ out feature spaces is defined by

$$\hat{r}_t = de_\theta(\tilde{r}_t) \quad \text{for } t \in \{1, \cdots, l\}$$

where $\theta \in \Theta_{de}$, and the network *de* is the decoder function. The decoder function takes risk-neutral process $\tilde{r}$ back to estimated realistic time-series $\hat{r}$.

Generator and discriminator: In the adversarial modeling framework two agents, the generator and the discriminator, are contesting with each other in a game-theoretic zero-sum game. Roughly speaking, the generator aims at generating samples such that the discriminator cannot distinguish whether the realizations were sampled from the target or the generator distribution. Different from other GAN-based models, the RiNN generator first outputs $\hat{\sigma}_{t,\gamma} \odot \hat{\epsilon}_{t,\eta}$ into the latent risk-neutral space instead of producing synthetic sequence directly. To ensure that the produced sequences retain causal ordering (i.e. output at each step can only depend on preceding information), we build the generator with the same structure as the encoder. Here we give the definition of the RiNN generator,

Definition 3 *(RiNN Generator)* Let $Z = (Z_t)_{t\in\mathbb{Z}}$ be $\mathbb{R}^m$-valued *i.i.d.* Gaussian noise, $g_h : \mathbb{R}^{m\times T} \times \Theta_g^{(h)} \to \mathbb{R}^{2n}$ and $g_\epsilon : \mathbb{R}^m \times \Theta_g^{(\epsilon)} \to \mathbb{R}^n$ be networks. Furthermore, let $\gamma \in \Theta_g^{(h)}$ and $\eta \in \Theta_g^{(\epsilon)}$ denote some parameters. A stochastic process $\hat{\tilde{r}}$, defined by

$$\hat{\tilde{r}} : \Omega \times \mathbb{Z} \times \Theta_g^{(h)} \times \Theta_g^{(\epsilon)} \to \mathbb{R}^n \tag{5}$$

$$(\omega, t, \gamma, \eta) \mapsto [\hat{\sigma}_{t,\gamma} \odot \hat{\epsilon}_{t,\eta} + \hat{\mu}_{t,\gamma}](\omega) \tag{6}$$

and

$$\begin{aligned} \hat{h}_t &:= g_h(Z_{(t-T):(t-1)}) \\ \hat{\sigma}_{t,\gamma} &:= |\hat{h}_{t,1:n}| \\ \hat{\mu}_{t,\gamma} &:= \hat{h}_{t,n+1:2n} \\ \hat{\epsilon}_{t,\eta} &:= g_\epsilon(Z_t) \end{aligned} \tag{7}$$

is called log-return risk-neutral process. The generator architecture defining the log-return risk-neutral process is called RiNN. Consistently, the neural process $\hat{\sigma}_{t,\gamma} := (\hat{\sigma}_{t,\gamma})_{t\in\mathbb{Z}}$, $\hat{\mu}_{t,\gamma} := (\hat{\mu}_{t,\gamma})_{t\in\mathbb{Z}}$, $\hat{r}_{f(t,\gamma)} := (\hat{r}_{f(t,\gamma)})_{t\in\mathbb{Z}}$ and $\hat{\epsilon}_{t,\eta} := (\hat{\epsilon}_{t,\eta})_{t\in\mathbb{Z}}$ are called volatility, drift, risk-neutral and innovation neural process, respectively.

Notice that $Z_{(t-T):(t-1)}$ can be sampled from a distribution of choice, and Z_t follows a stochastic process, here we assume that Z_t is a Wiener process. Finally, the discriminator function *d* determine whether the input data is from the risk-neutral space extracted by the encoder ($\tilde{r}_t$) or synthesized by the RiNN generator ($\hat{\tilde{r}}$). Here is our definition of the discriminator,

Definition 4 *(Discriminator)* Let $\widetilde{d}$: $\mathbb{R}^n \times \Theta_d \to \mathbb{R}$ be a network with parameters $\xi \in \Theta_d$ and $\sigma : \mathbb{R} \to [0, 1]$ defined by $x \mapsto 1/(1 + e^{-x})$ be the sigmoid function. A function $d : \mathbb{R}^n \times \Theta_d \to [0, 1]$ defined by $d : (r, \xi) \mapsto \sigma \circ \widetilde{d}_\xi(r)$ is called a discriminator.

Jointly learning to encode, generate, transfer and iterate: First, purely as a reversible mapping between real log-return space and neutral spaces, the encoder and decoder functions should be able to extract neutral representations $\tilde{r}$ from the real log-return sequence

r and accurately reconstruct $\hat{r}$ of the real market sequence from their neutral representations. Therefore, our first objective function is the reconstruction loss $\mathcal{L}_R$ defined by,

$$\mathcal{L}_R = \mathbb{E}_r\left[\sum_t \|r_t - \hat{r}_t\|_2\right]. \tag{8}$$

In *FinGAN*, the discriminator receives input from the risk-neutral sequence $\tilde{r}$ extracted by encoder and the risk-neutral sequence $\hat{\tilde{r}}$ synthesized by generator. First, the discriminator acts as a binary classifier, assigning a probability to each sample as a realization from the real risk-neutral distribution. This is as one would expect-that is, to maximize the likelihood that the discriminator will label $\tilde{r}$ as training data samples and $\hat{\tilde{r}}$ as generation samples,

$$\begin{aligned}\mathcal{L}_D &= \mathbb{E}[\ln(d(\tilde{r}))] + \mathbb{E}[\ln(1 - d(g(Z)))] \\ &= \mathbb{E}[\ln(d(\tilde{r}))] + \mathbb{E}[\ln(1 - d(\hat{\tilde{r}}))].\end{aligned} \tag{9}$$

However, relying solely on the discriminator's binary adversarial feedback may not be enough to motivate the generator to capture the distribution of risk-neutral sequences. To achieve this more efficiently, we propose an additional loss function $\mathcal{L}_S$ based on the volatility and innovation terms. The stochastic gradient can now be calculated on the loss of capturing the difference between $\sigma_t \odot \epsilon_t$ and $\tilde{\sigma_t} \odot \tilde{\epsilon_t}$ in the distributions, allowing the generator to improve its synthesis capabilities. Thus our third objective function is the supervised loss,

$$\mathcal{L}_S = D_{\mathrm{KL}}(\sigma_t \odot \epsilon_t \parallel \hat{\sigma_t} \odot \hat{\epsilon_t}), \tag{10}$$

where D_{KL} is the Kullback-Leibler divergence.

In sum, at any step in a training sequence, we assess the difference between the actual next-step risk-neutral latent vector (from the encoder function) and synthetic next-step risk-neutral latent vector (from the RiNN generator). While $\mathcal{L}_D$ pushes the RiNN generator to create risk-neutral sequences (evaluated by an imperfect adversary), $\mathcal{L}_S$ further ensures that it produces similar stepwise transitions (evaluated by ground-truth targets).

Optimization: The overall training objective is a min-max game played among the encoder, decoder, generator and discriminator. The first two components are trained on both the reconstruction and supervised losses,

$$\min_{\Theta_{en},\theta_{de}} (\lambda\mathcal{L}_S + \mathcal{L}_R), \tag{11}$$

where $\lambda \geq 0$ is a hyperparameter that balances the two losses.

Next, as *FinGAN* receives an error signal from both $\mathcal{L}_D$ and $\mathcal{L}_S$, we use another parameter γ to weight the ability to reconstruct vs. fooling the discriminator. That is, in addition to seeking a balancing point in the binary game of generator and discriminator, the generator will follow the encoder's style. Rather than applying γ to the entire model, we perform the weighting only when updating the parameter of the generator,

$$\theta_g \overset{+}{\leftarrow} -\nabla_{\theta_g}(\gamma\mathcal{L}_S + \mathcal{L}_D), \tag{12}$$

where $\gamma \geq 0$. Therefore, the generator and discriminator networks are trained adversarially as follows,

$$\min_{\Theta_g} \max_{\Theta_d} (\gamma \mathcal{L}_S + \mathcal{L}_D). \tag{13}$$

Notably, $\mathcal{L}_D$ is the determinant of how effectively the *FinGAN* is trained. If we consider $\mathcal{L}_D$ as a convex function of θ_g, then $\sup_D \mathcal{L}_D(\theta_g)$ has a unique global optima. Consequently with sufficiently small updates of θ_g, and θ_g converges to optima. This is equivalent to computing a gradient descent update for θ_g at the optimal discriminator given the corresponding generator. Pseudocode 1 show the pseudocode of *FinGAN*. We use Adam as the optimizer with learning rate of 1e-5 with $\lambda = 0.1$ and $\gamma = 0.1$. More architecture details can be found in Appendix.

Algorithm 1: Pseudocode of *FinGAN*

Input: λ, μ, batch size n_{batch}, learning rate α, dataset $\mathbf{R}$, receptive field size T
Initialize: $\theta_{en}, \theta_{de}, \theta_g, \theta_d$
// Prepare dataset
Extract dataset $\mathbf{r} = \left\{\mathbf{R}_{1:1+T}, \mathbf{R}_{2,2+T}, \cdots\right\}$ from $\mathbf{R}$ by a rolling window of size T
for $t = 0, 1, 2, \cdots$, *maximum number of iterations* **do**
  // (1) Map between Real Log-return Space and Risk Neutral Space
  Sample random mini-batch $\boldsymbol{r}$ from $\mathbf{r}$
  for $i = 1, \cdots, n_{batch}$ **do**
    $(\boldsymbol{\sigma}_i, \boldsymbol{\mu}_i, \boldsymbol{\epsilon}_i) = en(\boldsymbol{r}_i)$
    $\tilde{\boldsymbol{r}}_i = \boldsymbol{\sigma}_i \odot \boldsymbol{\epsilon}_i + \boldsymbol{\mu}_i$
    $\hat{\boldsymbol{r}}_i = de(\tilde{\boldsymbol{r}}_i)$
  end

  // (2) Generate Synthetic Risk Neutral Sequence
  Sample $\mathbf{z}_{1,1:T}, \cdots, \mathbf{z}_{n_{batch},1:T} \overset{i.i.d}{\sim} \mathcal{Z}$
  for $i = 1, \cdots, n_{batch}$ **do**
    $(\hat{\boldsymbol{\sigma}}_i, \hat{\boldsymbol{\mu}}_i, \hat{\boldsymbol{\epsilon}}_i) = g(\mathbf{z}_i)$
    $\hat{\tilde{\boldsymbol{r}}}_i = \hat{\boldsymbol{\sigma}}_i \odot \hat{\boldsymbol{\epsilon}}_i + \hat{\boldsymbol{\mu}}_i$
  end

  // (3) Distinguish between Real and Synthetic Sequence
  for $i = 1, \cdots, n_{batch}$ **do**
    $y_i = d(\tilde{\boldsymbol{r}}_i)$
    $\hat{y}_i = d(\hat{\tilde{\boldsymbol{r}}}_i)$
  end

  // (4) Compute Loss Functions
  $\mathcal{L}_R = \frac{1}{n_{batch}} \sum_{i=1}^{n_{batch}} \left[\sum t \|\boldsymbol{r}_{i,t} - \hat{\boldsymbol{r}}_{i,t}\|_2\right].$
  $\mathcal{L}_D = \frac{1}{n_{batch}} \sum_{i=1}^{n_{batch}} \left[\ln y_i + \ln(1 - \hat{y}_i)\right]$
  $\mathcal{L}_S = D_{KL}[N(\mathbb{E}[\boldsymbol{\sigma} \odot \boldsymbol{\epsilon}], \Sigma[\boldsymbol{\sigma} \odot \boldsymbol{\epsilon}]) \parallel N(\mathbb{E}[\hat{\boldsymbol{\sigma}} \odot \hat{\boldsymbol{\epsilon}}], \Sigma[\hat{\boldsymbol{\sigma}} \odot \hat{\boldsymbol{\epsilon}}])]$

  // (5) Update $\theta_{en}, \theta_{de}, \theta_g, \theta_d$ via Stochastic Gradient Descent (SGD)
  $\theta_{en} = \theta_{en} - \nabla_{en}(\lambda \mathcal{L}_S + \mathcal{L}_R)$
  $\theta_{de} = \theta_{de} - \nabla_{de} \mathcal{L}_R$
  $\theta_d = \theta_d + \nabla_d \mathcal{L}_D$
  $\theta_g = \theta_g - \nabla_g(\gamma \mathcal{L}_S + \mathcal{L}_D)$

  if $\Delta \mathcal{L}_D <$ *precision value* **then**
    break;
  end
end

Theoretical basis

Considering a one-dimensional log-return neural process, where the innovation neural process is constrained to represent a standard normal distributed random variable.

$$\mathrm{r}_{t,\theta} = \sigma_{t,\theta}\epsilon_{t,\theta} + \mu_{t,\theta} \tag{14}$$

where, $\epsilon_{t,\theta} \sim \mathcal{N}(0,1)$ for all $t \in \mathbb{Z}$.

Then, the underlying stock prices are defined recursively by Eq. 15,

$$\mathrm{S}_{t,\theta} = \mathrm{S}_{t-1,\theta}\ \exp(\mathrm{r}_{t,\theta}) \qquad \text{for all } t \in \mathbb{N} \tag{15}$$

where $\mathrm{S}_{0,\theta} = \mathrm{S}_0$ denotes the current price of the underlying stock.

Moreover, we assume a constant interest rate r_f and denote the discounted stock price $(\mathrm{S}^{(d)}_{t,\theta})_{t\in\mathbb{N}}$ in Eq. 16,

$$\mathrm{S}^{(d)}_{t,\theta} := \frac{\mathrm{S}_{t,\theta}}{\exp(\mathrm{r}_f t)} \tag{16}$$

The discounted asset price is given in Eq. 17,

$$\mathrm{S}^{(d)}_{t,\theta} = \mathrm{S}^{(d)}_{t-1,\theta}\ \exp(\mathrm{r}_{t,\theta} - \mathrm{r}_f) \tag{17}$$

As we cannot value options under a log-return neural process, but need to convert it to its risk-neutral distribution. Given a risk-neutral probability space $(\Omega, \mathcal{F}, \mathbb{Q})$ and information filtration $\{\mathcal{F}_t\}$, the discounted stock price process is a martingale. Therefore, we have,

$$\begin{aligned} \mathrm{E}^{\mathbb{Q}}[\mathrm{S}^{(d)}_{t,\theta}|\mathcal{F}_{t-1}] &= \mathrm{E}^{\mathbb{Q}}[\mathrm{S}^{(d)}_{t-1,\theta}\ \exp(\mathrm{r}_{t,\theta} - \mathrm{r}_f)|\mathcal{F}_{t-1}] \\ &= \mathrm{S}^{(d)}_{t-1,\theta}\ \exp(-\mathrm{r}_f)\ \mathrm{E}^{\mathbb{Q}}[\exp(\sigma_{t,\theta}\epsilon_{t,\theta} + \mu_{t,\theta})|\mathcal{F}_{t-1}] \end{aligned} \tag{18}$$

We denote the conditional expectation given in Eq. 18 by $h(\sigma_{t,\theta}, \mu_{t,\theta}) := \mathrm{E}^{\mathbb{Q}}[\exp(\sigma_{t,\theta}\epsilon_{t,\theta} + \mu_{t,\theta})|\mathcal{F}_{t-1}]$. As the $\mathcal{F}_{t-1}$-measurable volatility and drift neural process, $\epsilon_{t,\theta} \sim \mathcal{N}(0,1)$ and the independent of $\mathcal{F}_{t-1}$, $h(\sigma_{t,\theta}, \mu_{t,\theta})$ can be calculated explicitly:

$$\begin{aligned} h(\sigma_{t,\theta}, \mu_{t,\theta}) =& \mathrm{E}^{\mathbb{Q}}[\exp(\sigma_{t,\theta}\epsilon_{t,\theta} + \mu_{t,\theta})] \\ =& \exp\left(\mu_{t,\theta} + \frac{\sigma^2_{t,\theta}}{2}\right) \end{aligned} \tag{19}$$

Now, we denote the risk-neutral log return neural process by $\widetilde{\mathrm{r}}_{t,\theta} := \mathrm{r}_{t,\theta} - \ln(h(\sigma_{t,\theta}, \mu_{t,\theta})) + \mathrm{r}_f$, and the risk-neutral log return neural process is given by:

$$\widetilde{\mathrm{r}}_{t,\theta} = \sigma_{t,\theta}\epsilon_{t,\theta} - \frac{\sigma^2_{t,\theta}}{2} + \mathrm{r}_f \tag{20}$$

and the discounted risk-neutral price process is given by:

$$\widetilde{S}_{t,\theta} = \widetilde{S}_{t-1,\theta} \exp\left(\sigma_{t,\theta}\epsilon_{t,\theta} - \frac{\sigma_{t,\theta}^2}{2}\right) \tag{21}$$

in particular, the discounted risk-neutral spot price process is given by:

$$\widetilde{S}_{t,\theta} = S_0 \exp\left(\sum_{s=1}^{t}\left(\sigma_{t,\theta}\epsilon_{t,\theta} - \frac{\sigma_{t,\theta}^2}{2}\right)\right) \tag{22}$$

Interest rate

The interest rate in this study is assumed as a constant r_f, and all interest rate data employed is obtained from the China Central Depository and Clearing Co., Ltd.. The time-series of the risk-free interest rates are extracted from the Chinese treasury bond and cover maturities from 3 months to 10 years on a daily basis. We obtain through Hermite interpolation the complete term structure of spot rates at any time.

Credit risk

We account for credit risk in the spirit of Tsiveriotis and Fernandes (1998) and discount the cash flows subject to credit risk with the appropriate interest rate. We calibrate the probability of default from the spread between the risk-free interest rate and the yield of company bond. If the issuer's bond yield is not available, we can use the yield for the company bond with the same rating. Coupon payments, the redemption payment κN, the call price in the event of a conditional redemption C_t and the put price in the event of a repurchase P_t are subject to credit risk. The stock price S_t, on the other hand, is not and should therefore be discounted with the risk-free interest rate.

Data and experiment

In this section, we empirically evaluate our *DeepPricing* model by the data in the Chinese convertible bond market. We examine the Chinese convertible bond market for three main reasons. Firstly, China has the fastest growing convertible bond market in the past decade, the number of convertible issuance has increased from 8 in 2010 to 186 in 2020 and the scale has increased from 71,730.00 CNY million in 2010 to 230,064.20 CNY million in 2020. Secondly, some special terms of the Chinese convertible bond, such as the *Conditional Redemption Term*, *Conversion Price Revision Terms*, cause huge difficulty in the valuation, thus, there is not much literature focusing on the Chinese convertible bond market. Thirdly, due to the unique trading constraints such as price-limit rules and short-sale restrictions in the Chinese stock market, any assumptions about the distribution of the underlying stock return process cannot completely conform to its real return distributions, thus the alternative data-driven path simulator is much more needed.

This section is divided into five parts. "Data description" section gives a brief introduction of the descriptive statistics of convertible bond data. "Baseline methods" section introduces several baseline models of generating dynamic underlying stock return process. "Comparisons with different stock return generators" section reviews

major statistical properties of the underlying stock return process and compares the statistical properties of the generated underlying stock return process between the *FinGAN* and other baseline generation models. "Model performance and Robustness test" section provides the main empirical results and robustness tests on convertible bonds pricing performances across *DeepPricing* and baseline valuation models. "Analysis of mispricing" section further analyzes the potential influencing factors on the mispricing of convertible bonds.

Data description

For the empirical investigations, we obtain daily returns and the basic terms for all Chinese convertible bonds listed on the Shanghai and Shenzhen stock exchanges from the Wind Database. Besides, to ensure the consistency and reliability of the data, we use Bloomberg Database for cross-validation. Within this sample, those that were non-publicly raised and lacked an active underlying common stock were excluded from the sample. Based on these criteria, our data sample covers a total of 579 convertible bonds and 125,306 observations from January 01, 2010 to June 30, 2021.

To provide additional details, the sample is divided into several categories according to either the equity component levels or market states. Following Burlacu (2000), the equity component level is classified by Δ (defined in Eq. 23), the sensitivity of the convertible bond value to its underlying common stock. And the debt-liked convertible bonds, the balanced convertible bonds, and the equity-liked convertible bonds is determined by its belongingness to the intervals [0, 0.33]; [0.33, 0.66]; and [0.66, 1], respectively.

$$\Delta = e^{-\delta\tau} N\left(\frac{\ln(\mathrm{S}_t/\mathrm{K}_t) + (\mathrm{r}_f - \delta + \sigma^2/2)\tau}{\sigma\sqrt{\tau}}\right) \tag{23}$$

where S_t is the current price of the underlying stock, K_t is the conversion price, r_f is the risk-free rate estimated from Chinese treasury bonds on the issue date, σ is the standard deviation of the continuously compounded underlying stock returns, τ is the number of years to maturity, δ is the continuously compounded dividend yield, and $N(.)$ is the cumulative probability under a standard normal distribution function. The market states is classified by the bull market (including subperiod from January 01, 2014 to June 12, 2015 and subperiod from January 01, 2019 to June 30, 2021), the bear market (including subperiod from January 01, 2010 to December 31, 2013; subperiod from June 15, 2015 to January 29, 2016; subperiod from January 01, 2018 to December 31, 2018) and the direction-less market (including subperiod from February 01, 2016 to December 31, 2017).

Table 2 reports some key summary statistics for the sample. Panel A summarizes the statistics of the whole sample, Panels B.1, B.2, B.3 provides the information on the subsamples by the equity component levels of convertible bonds, and Panels C.1, C.2, C.3 provides the information on the subsamples across different convertible bond market states.

Panel A of Table 2 shows that the mean maturity of all convertible bonds at issuance is 5.93 years with 6-years being the longest maturity. Industry, material, and information technology accounted for 145 (25.04%), 129 (22.28%), and 89 (15.37%) of the bonds, respectively. Consumer discretionary, healthcare, and consumer stables accounted for

70 (12.09%), 42 (7.25%), and 37 (6.39%) bonds. Financial corporations accounted for 34 (5.87%) of the bonds, and the remaining 34 bonds were issued by firms from other industries including public utilities (20 or 3.45%), energy (7 or 1.21%), and real estate (6 or 1.04%)[3]. The highest credit rating in our sample of bonds was AAA (15.13% of 125,306 observations) and the lowest was A (0.24% of 125,306 observations). Notice that contrary to the US convertible market[4], due to the strict issuance conditions, there is almost no credit risk in the Chinese convertible bond market. The average convertible bond can be converted at a conversion price of 14.70 CNY per share and a conversion premium[5] of 26.38%. The mean total issuance is approximately 259,263.94 CNY million. The daily average trading amount and the turnover rate is 103.07 CNY million and 7.66%, respectively, however, the standard deviation of daily average amount and the turnover rate is 153.90 CNY million and 15.23%, which indicate that the liquidity of individual bonds in the Chinese convertible bond market is very different. Panels B.1, B.2 and B.3 show that the equity-liked convertible bonds have relatively lower conversion premium (Brown et al. 2012), higher underlying stock volatility, higher liquidity (higher daily average amount and turnover rate). Whereas the debt-liked convertible bonds exactly show the opposite features. Moreover, Panels C.1, C.2 and C.3 show that the average conversion premium in the bull market is lower than bear market, which indicates that the convertible bond is more equity-liked in the bull market. Meanwhile, convertible bonds in the bull market are more liquid than in the bear market.

Baseline methods

As we mentioned in "The DeepPricing model" section, the most important input in convertible bonds valuation framework is the simulation of underlying stock return process. In this section, we first introduce three commonly used traditional models to generate underlying stock return dynamics, i.e., the Black-Scholes (BS) model, the constant elasticity of variance (CEV) model, the GARCH model. In addition, we also consider two state-of-the-art networks, i.e. multilayer perceptron (MLP) and LSTM, to solve the time-series simulation problem. For fair comparison, we use the same architecture as the *FinGAN* model shown in Fig. 2 and the MLP and LSTM are only used to instead TCN networks.

BS model BS model assumes the underlying stock price S_t follows the geometric Brownian motion in Eq. 24. The volatility is constant and are independent of time and the current S_t.

$$dS_t = \mu S_t dt + \sigma S_t dB_t \qquad (t > 0) \tag{24}$$

The volatility σ is measured by the standard deviation defined in Eq. 25, estimated on a historical basis, using the time-series data of the underlying stock. The volatility for each convertible bond is calculated using daily individual stock returns for 20 trading days prior to the first real-time trade data reported to WIND and is assumed to be constant.

[3] Not reported in the table.

[4] US convertible market is more accessible for issuers who have difficulty entering the traditional bond market due to restrictive rating requirements (Batten et al. 2018).

[5] The conversion premium measures the excess of the conversion price over the stock price at issuance as a percentage of the stock price.

Table 2 Summary statistics of the sample

	Mean	SD	Min	Q1	Median	Q3	Max
Panel A. All convertible bonds							
Maturity (years)	5.93	1.15	1.00	4.00	5.00	6.00	6.00
Credit rating	2.72	0.97	1.00	2.00	3.00	3.00	6.00
Conversion price (CNY)	14.70	14.79	2.27	6.88	9.99	16.83	158.00
Conversion premium (%)	26.38	31.22	−34.22	7.61	18.06	33.12	356.43
Underlying stock volatility	0.40	0.15	0.07	0.29	0.38	0.49	1.30
Total issuance (CNY' Mil.)	259,263.94	596,140.28	18,500.00	62,000.00	98,000.00	215,300.00	5,000,000.00
Daily average amount (CNY' Mil.)	103.07	153.90	3.06	23.75	46.25	109.89	1,440.43
Daily average turnover (%)	7.66	15.23	0.34	1.66	3.46	7.15	148.99
Panel B.1. Equity-liked convertible bonds							
Maturity (years)	5.72	0.98	1.00	5.00	5.00	6.00	6.00
Credit rating	2.86	0.94	1.00	2.00	3.00	3.00	6.00
Conversion price (CNY)	18.12	19.96	2.27	6.98	11.20	19.75	158.00
Conversion premium (%)	8.65	17.41	−34.22	0.27	4.53	11.17	297.58
Underlying stock volatility	0.49	0.16	0.10	0.39	0.49	0.59	1.30
Total issuance (CNY' Mil.)	201,029.91	410,261.08	19,157.00	53,800.00	94,183.00	180,000.00	4,000,000.00
Daily average amount (CNY' Mil.)	211.86	379.06	5.24	50.83	93.30	198.31	3,002.40
Daily average turnover (%)	16.32	37.03	0.40	3.24	5.37	12.40	408.09
Panel B.2. Balanced convertible bonds							
Maturity (years)	5.89	1.02	1.00	4.00	5.00	6.00	6.00
Credit rating	2.72	1.00	1.00	2.00	3.00	3.00	6.00
Conversion price (CNY)	13.56	12.19	2.27	6.15	9.71	16.72	83.85
Conversion premium (%)	20.32	18.83	−5.50	11.59	16.95	24.06	344.59
Underlying stock volatility	0.37	0.11	0.10	0.30	0.37	0.45	0.94
Total issuance (CNY' Mil.)	255,681.93	547,929.89	18,500.00	60,000.00	98,000.00	230,000.00	4,000,000.00
Daily average amount (CNY' Mil.)	81.67	268.66	2.04	14.60	27.05	54.07	3,182.42
Daily average turnover (%)	5.73	18.08	0.20	1.23	1.93	4.24	263.91
Panel B.3. Bond-liked convertible bonds							
Maturity (years)	5.62	1.24	1.00	3.00	4.00	5.00	6.00
Credit rating	2.61	0.97	1.00	2.00	3.00	3.00	6.00
Conversion price (CNY)	12.49	9.79	2.27	7.04	9.76	14.74	81.49
Conversion premium (%)	48.90	36.75	0.27	25.98	38.26	58.97	356.43
Underlying stock volatility	0.32	0.11	0.07	0.24	0.30	0.38	0.86
Total issuance (CNY' Mil.)	318,043.98	760,364.97	18,500.00	71,700.00	100,000.00	241,300.00	5,000,000.00
Daily average amount (CNY' Mil.)	3.51	21.75	0.00	0.24	0.59	1.58	2,973.45

Table 2 (continued)

	Mean	SD	Min	Q1	Median	Q3	Max
Daily average turnover (%)	2.41	7.06	0.07	0.60	0.84	1.41	83.03
Panel C.1. Bull market							
Maturity (years)	5.62	1.18	1.00	4.00	5.00	6.00	6.00
Credit rating	2.81	0.96	1.00	2.00	3.00	3.00	6.00
Conversion price (CNY)	15.20	15.81	2.27	6.78	10.29	16.81	158.00
Conversion premium (%)	25.49	32.05	−34.22	6.76	17.16	31.32	356.43
Underlying stock volatility	0.41	0.15	0.10	0.30	0.39	0.50	1.30
Total issuance (CNY' Mil.)	213,281.06	499,770.47	18,500.00	59,575.00	92,800.00	187,522.00	5,000,000.00
Daily average amount (CNY' Mil.)	110.10	167.43	1.59	24.41	47.07	114.29	1,440.43
Daily average turnover (%)	8.05	15.79	0.21	1.72	3.48	7.41	149.78
Panel C.2. Direction-less market							
Maturity (years)	5.87	0.96	2.00	5.00	5.00	6.00	6.00
Credit rating	2.56	0.90	1.00	2.00	3.00	3.00	4.00
Conversion price (CNY)	11.87	6.73	4.26	7.74	9.40	15.25	45.48
Conversion premium (%)	32.78	20.72	−4.56	16.24	29.65	46.85	114.30
Underlying stock volatility	0.32	0.14	0.11	0.22	0.29	0.39	0.83
Total issuance (CNY' Mil.)	297,016.59	524,006.69	18,500.00	81,366.00	120,000.00	410,558.00	3,000,000.00
Daily average amount (CNY' Mil.)	77.54	77.66	7.58	16.45	59.17	101.17	301.45
Daily average turnover (%)	4.79	5.02	0.85	1.19	2.72	6.81	23.98
Panel C.3. Bear market							
Maturity (years)	5.74	1.05	1.00	4.00	5.00	6.00	6.00
Credit rating	2.38	1.00	1.00	1.00	3.00	3.00	4.00
Conversion price (CNY)	13.22	10.99	2.40	6.88	9.15	17.47	81.49
Conversion premium (%)	28.63	29.39	−10.49	9.74	19.58	36.63	231.42
Underlying stock volatility	0.35	0.14	0.07	0.26	0.34	0.43	1.08
Total issuance (CNY' Mil.)	453,004.13	892,501.73	18,500.00	71,700.00	140,000.00	340,000.00	4,000,000.00
Daily average amount (CNY' Mil.)	59.67	125.40	2.06	9.85	23.72	52.33	1,028.21
Daily average turnover (%)	2.93	4.15	0.39	0.89	1.51	3.17	26.32

Table 2 reports the summary statistics of the observed characteristics for the sample of 579 convertible bonds. Maturity is the convertible bond's time to maturity at issuance in years. Rating information is collected from WIND. The numerical values for credit ratings are: $AAA = 1$, $AA+ = 2$, $AA = 3$, $AA- = 4$, $A+ = 5$, $A = 6$. The conversion price is the prespecified price per share of the underlying stock when conversion takes place. Conversion premium measures the percentage by which the conversion price exceeds the underlying stock price. Initial issuance is the convertible bond's issuance size (face value). Daily average amount and turnover is the average daily trading amount and turnover for convertible bond *i*. Panel A reports the statistics of the whole sample, Panels B.1, B.2, B.3 reports the statistics categorized by the equity component levels of convertible bonds, and Panels C.1, C.2, C.3 reports the statistics categorized by market states. The sample period is from January 01, 2010 through June 30, 2021 and includes 125,306 observations

$$\sigma = \sqrt{\frac{1}{\mathrm{N}-1}\sum_{t=1}^{\mathrm{N}}(\mathrm{R}_t - \bar{\mathrm{R}})^2} \tag{25}$$

CEV model CEV model extends the BS model to include the observed inverse dependence of volatility and implied volatility skew (Christie 1982; Cox 1996). The CEV model assumes the underlying stock price S_t take the following form:

$$d\mathrm{S}_t = \mu \mathrm{S}_t dt + \sigma \mathrm{S}_t^{\frac{\beta}{2}} d\mathrm{B}_t \qquad (t > 0, 0 \leq \beta < 2) \tag{26}$$

The value of β is estimated via the following equation:

$$\ln|\ln\frac{\mathrm{S}_{t+1}}{\mathrm{S}_t}| = \nu + \kappa \ln \mathrm{S}_t + \epsilon_t \tag{27}$$

where $\nu = \ln\sigma$ and $\kappa = \frac{\beta-2}{2}$. The β for each convertible bond's issuer is estimated from the daily stock returns of 20 trading days prior to the first real-time trade price reported to WIND, which is similar to the estimation of volatility discussed earlier.

GARCH (1,1) model GARCH (1,1) model is the simplest way to extend the BS model's constant volatility assumption to GARCH (1,1), in order to capture the volatility patterns present in the data, in particular volatility clustering (Bollerslev (1986)). Following Bollerslev (1986) and Duan (1995), the conditional variance of the GARCH (1,1) evolves as

$$\sigma_t^2 = \alpha_0 + \alpha_1 \epsilon_{t-1}^2 + \beta_1 \sigma_{t-1}^2 \tag{28}$$

where $\alpha_0 > 0, \alpha_1 \geq 0, \beta_1 \geq 0$ and the ϵ_t are the return residuals, in which $\epsilon_t = \sigma_t \mathrm{Z}_t$ with $\mathrm{Z}_t \sim \mathrm{N}(0,1)$. σ is estimated from the daily underlying stock returns of 20 trading days prior to the first real-time trade price reported to WIND.

FinGAN-MLP model In the FinGAN-MLP model, we use the MLP networks to replace the original TCN networks in *FinGAN*. For a neuron in the MLP, the output o_i is defined by Eq. 29:

$$o_i = \phi\left(\sum_{j=1}^{d}(r_i w_{ij} + b_j)\right) \tag{29}$$

where d is the length of the input r_t, r_i is the single instance of the input vector, and b_j and w_{ij} are the bias and weights associated with each r_i.

FinGAN-LSTM model In the FinGAN-LSTM model, we use the LSTM networks to replace the original TCN networks in *FinGAN*. At each time step, an LSTM maintains a hidden vector h and a memory vector c responsible for controlling state updates and outputs. More concretely, the operations performed by an LSTM unit at time step t as follows:

$$i_t = \sigma(U_i \mathrm{r}_t + W_i h_{t-1} + b_i) \tag{30}$$

$$f_t = \sigma\left(U_g \mathrm{r}_t + W_g h_{t-1} + b_g\right) \tag{31}$$

$$c_t^* = \tanh\left(U_c \mathrm{r}_t + W_c h_{t-1} + b_c\right) \tag{32}$$

$$c_t = g_t \odot c_{t-1} + i_t \odot c_t^* \tag{33}$$

$$o_t = \sigma\left(U_o \mathrm{r}_t + W_o h_{t-1} + b_o\right) \tag{34}$$

where r_t denotes the input, W_* and U_* are weight matrices, b_* are the vectors of bias term, σ is the sigmoid function, and the operator $\odot$ denotes component-wise multiplication. Finally, the output of the memory cell is calculated by

$$h_t = o_t \odot \tanh(c_t) \tag{35}$$

For more details on LSTM processes, see Zhang et al. (2019).

Comparisons with different stock return generators

In this section, we take *Sun Paper* (stock code: 002078.SZ), the underlying stock of the *Sun Convertible Bond* (convertible bond code: 128029.SZ), as an example to compare the ability of different generation models to characterize the main statistical properties of the underlying stock returns process. First, stylized facts of real financial time-series (Cont 2001; Chakraborti et al. 2011; Takahashi et al. 2019) are reviewed to assess the quality of generated data. Second, the reproducibility of statistical properties of different generators is analyzed and compared with real financial time-series. Finally, the robustness of training process of GAN-based models is reported.

Statistical properties of financial time-series

The main statistical properties of real stock returns including the linear unpredictability, the fat-tailed distribution, the volatility clustering, the leverage effects, the coarse-fine volatility correlation, and the gain/loss asymmetry (in the first line of Fig. 4 and Table 3), we give a short introduction of each in turn.

Linear unpredictability (LUI) linear unpredictability is quantified by the diminishing autocorrelation function of stock returns, defined in Eq. 36. Empirically, there is no autocorrelation in daily frequency return series (Chakraborti et al. (2011)).

$$\mathrm{Corr}\left(\mathrm{r}_t, \mathrm{r}_{t+k}\right) = \frac{\mathrm{E}\left[\left(\mathrm{r}_t - \bar{\mathrm{r}}\right)\left(\mathrm{r}_{t+k} - \bar{\mathrm{r}}\right)\right]}{\sigma^2} \approx 0, \quad \textit{for } k \geq 1 \tag{36}$$

where $\bar{\mathrm{r}}$ and σ are the mean and the standard deviation of the stock return. Figure 4(i-a) shows the decay of the autocorrelation of the *Sun Paper* in daily scale.

Fat-tailed distribution (FTD) fat-tailed distribution is characterized by a higher probability density of outliers than the normal distribution. The probability of distribution $\Pr(\mathrm{r}_t)$ consistently has a power-law decay in the tails defined in Eq. 37 (Liu et al. 1999). Empirically, for normal distribution the power law asymptotic exponent $\alpha \geq 5$, and real stock return distribution range $3 \leq \alpha < 5$. The positive-tail ($\alpha = 3.4924$) of the *Sun Paper* of 3, 556 data points in Fig. 4(i-b) is observed.

$$\Pr(\mathrm{r}_t) \propto \mathrm{r}_t^{-\alpha} \tag{37}$$

Volatility clustering (VC) volatility clustering refers to the fact that the large/small stock return fluctuations tend to cluster together temporally, which indicates the presence of the long-range temporal dependence in financial time-series. Quantitatively, volatility clustering is characterized with the power law decay of the autocorrelation function of the absolute stock returns, defined in Eq. 38 (Cont 2007). The slow and power decay up to $k \approx 10^2$ ($\beta = 1.1194$) of the *Sun Paper* of 3,556 data points in Fig. 4(i-c) is observed.

$$\mathrm{Corr}\big(|\mathrm{r}_t|, |\mathrm{r}_{t+k}|\big) \propto k^{-\beta} \tag{38}$$

Leverage effect (LE) Leverage effects refer to the tendency that the past stock return has a correlation with future volatility[6]. Quantitatively, leverage effect is characterized with the lead-lag correlation function defined in Eq. 39 (Bouchaud et al. 2001; Qiu et al. 2006). In the case of the *Sun Paper*, the positive correlation is found for $1 < k < 10$ as shown in Fig. 4(i-d).

$$L(k) = \frac{\mathrm{E}[\mathrm{r}_t|\mathrm{r}_{t+k}|^2] - \mathrm{r}_t|\mathrm{r}_t|^2}{\mathrm{E}[|\mathrm{r}_t|^2]^2} \tag{39}$$

Coarse-fine volatility correlation (CFVC) Coarse-fine volatility correlation refer to fine volatility has the power of predicting coarse volatility. Quantitatively, coarse-fine volatility correlation is characterized with the negative asymmetry of the lead-lag correlation defined in Eq. 40 (Müller et al. 1997; Gavrishchaka and Ganguli (2003).

$$\Delta\rho_c f^\tau(k) = \rho_c f^\tau(k) - \rho_c f^\tau(-k) \tag{40}$$

where the lead-lag correlation of two different time scales volatility $\rho_c f^\tau(k)$ is defined in Eq. 41,

$$\rho_c f^\tau(k) = \mathrm{Corr}(v_c^\tau(t+k), v_f^\tau(t)) \tag{41}$$

$v_c^\tau(t) = |\sum_{i=1}^{\tau} r_{t-i}|$ is coarse volatility and $v_f^\tau(t) = \sum_{i=1}^{\tau} |r_{t-i}|$ is fine volatility.

The negative $\Delta\rho_c f^\tau(k)$ indicates that fine volatility has the power of predicting coarse volatility. Figure 4(i-e) shows the coarse-fine volatility correlation $\rho_c f^\tau(k)$ in blue points and the lead-lag correlation asymmetry $\Delta\rho_c f^\tau(k)$ in orange points. The asymmetry is present in the *Sun Paper* as the value deviates from the zero level indicated by the black dashed line.

Gain/loss asymmetry (GLA) Gain/loss asymmetry refers to the speed of the stock price fall is faster than the stock price rise. Quantitatively, gain/loss asymmetry is characterized with the probability distribution of $T^t_{\mathrm{wait}}(\theta)$ relating to the speed of stock price movement to reach the certain positive and negative change $\pm\theta$, defined in Eq. 42 (Jensen et al. 2003).

$$T^t_{\mathrm{wait}}(\theta) = \begin{cases} \inf\{k|\mathrm{r}_{[t,t+k]} \geq \theta, k > 0\} & (\theta > 0) \\ \inf\{k|\mathrm{r}_{[t,t+k]} \leq \theta, k > 0\} & (\theta < 0) \end{cases} \tag{42}$$

[6] Notice that this property is market dependent (Qiu et al. (2006)). While the negative correlation (leverage effect) is observed in German DAX, the positive correlation (anti-leverage effect) is detected in Chinese market.

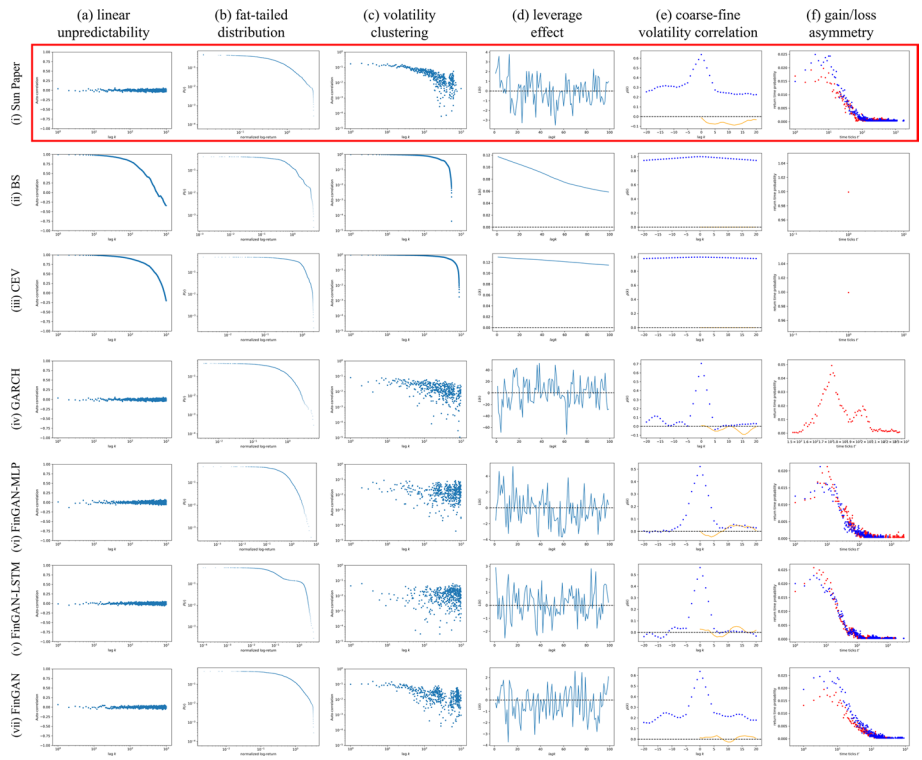

Fig. 4 Statistical properties for the return process of the *Sun Paper* and return process generated by BS, CEV, GARCH, FinGAN-MLP, FinGAN-LSTM and *FinGAN* models. (**a**) Linear unpredictability is shown as the zero level of the auto-correlation function of the price return is at zero level for all lags. (**b**) Fat-tailed distribution is demonstrated by the power-law decay of the tails of the probability distribution. (**c**) Volatility clustering is expressed by the slow decay of the auto-correlation function for the absolute values of the price return. (**d**) Leverage effects are shown as the lead-lag correlation of the price return and the price volatility. (**e**) Coarse-fine volatility correlation is shown as the lead-lag correlation of the coarse and the fine volatility. (**f**) Gain/loss asymmetry is shown in the difference of the probability distributions for the time-step required to reach a certain positive (red) and negative (blue) price change. The sample period is from November 16, 2006 through June 30, 2021 and includes 3,556 observations

Figure 4(i-f) shows the probability distribution of $T^t_{\text{wait}}(\theta = 0.1)$ in red and $T^t_{\text{wait}}(\theta = -0.1)$ in blue for the *Sun Paper*. The peak of the positive returns comes before the peak of negative returns, indicating the presence of asymmetry in price up/down.

Experiment results

The reproducibility of statistical properties with different models are summarized in Fig. 4 and Table 3[7]. The empirical results show that the time-series generated by the *FinGAN* model satisfies all six major statistical properties of the *Sun Paper* return series. In comparison, the traditional generator such as BS, CEV, GARCH outputs time-series that satisfies the stylized facts of the fat-tailed distribution, however, does not successfully reproduce the the leverage effect, the asymmetry in coarse-fine volatility correlation and the gain/loss asymmetry. While for more state-of-art approaches such as FinGAN-MLP and FinGAN-LSTM generators outputs time-series also satisfy major statistical

[7] For fair comparison, the FinGAN-MLP and FinGAN-LASM models have been trained with the same optimizer (Adam) and learning rate of 1e-5 as FinGAN.

Table 3 Reproducibility of statistical properties with different generators

Model	σ	LU	FTD	VC	LE	CFVC		GLA	
		$l(k)$	α	β	$L(k)$	$\rho^{\tau}_{cf}(k)$	$\Delta\rho^{\tau}_{cf}(k)$	T^{t}_{wait} $(\theta = 0.1)$	$T^{t}_{\text{wait}}(\theta = -0.1)$
Sun Paper	0.0293	[−0.0581, 0.0603]	3.4924	1.1194	[−3.7770, 3.5193]	[0.0949, 0.6391]	[−0.0883, 0.0321]	6	7
BS	1.4418	[−0.3411, 0.9979]	23.6205	1.3601	[0.1566, 0.2481]	[0.8256, 1.0000]	[0.0000, 0.0000]	0	0
CEV	0.9011	[−0.2036, 0.9988]	5.5313	1.3448	[0.1150, 0.1298]	[0.9037, 1.0000]	[0.0000, 0.0000]	0	0
GARCH	0.0005	[−0.0582, 0.0604]	3.4920	1.0852	[−72.3026, 51.9073]	[−0.0376, 0.7069]	[−0.0897, 0.0230]	0	25
FinGAN-MLP	0.0347	[−0.0711, 0.0656]	5.4085	1.0844	[−3.7114, 5.0010]	[−0.0714, 0.6410]	[−0.0652, 0.0843]	6	10
FinGAN-LSTP	0.0312	[−0.0647, 0.0620]	6.4557	1.0835	[−3.1369, 3.1684]	[−0.0777, 0.6003]	[−0.0821, 0.0825]	3	3
FinGAN	0.0288	[−0.0627, 0.0593]	4.8038	1.1061	[−2.7933, 4.3075]	[−0.0265, 0.5292]	[−0.0865, 0.0567]	6	7

Table 3 reports the statistical properties for the daily stock returns of the *Sun Paper* and different stock return generators. LU stands for linear unpredictability, $l(k)$ denotes the interval of the diminishing auto-correlation defined in Eq. 36. FTD stands for fat-tailed distribution, α is the exponent of the power-law decay defined in Eq. 37. VC stands for volatility clustering, β is the exponent of the power-law decay of the auto-correlation function defined in Eq. 38. LE stands for leverage effect, $L(k)$ is the range of lead-lag correlation function defined in Eq. 39. CFVC stands for coarse-fine volatility correlation, $\rho^{\tau}_{cf}(k)$ is defined in Eq. 41, and $\Delta\rho^{\tau}_{cf}(k)$ is defined in Eq. 40. GLA stands for gain/loss asymmetry, $T^{t}_{\text{wait}}(\theta)$ is defined in Eq. 42. The sample period is from November 16, 2006 through June 30, 2021 and includes 3,556 observations

properties, however, the *FinGAN* model shows more high-quality synthetic data in comparison to real data set based on both visualization (in Fig. 4) and the parameter scope (in Table 3).

Robustness of training

It was reported that GANs are difficult to converge during the training process (Salimans et al. 2016), in this section, the robustness of different GAN-based models are tested. Figure 5 shows the loss of the generator and the discriminator in FinGAN-MLP, FinGAN-LSTM and *FinGAN*, respectively. With the same optimizer and learning rate, the *FinGAN* model converges faster than others and converges toward a minimum as the network trains. In comparison, the loss of FinGAN-MLP and FinGAN-LSTM models do not show a stable trend as iterations increase.

Model performance and Robustness test

We conduct empirical studies to discuss the convertible bonds pricing results produced by *DeepPricing* and other baseline valuation models. In order to be more comparable with baseline models, we use the uniform pricing framework as the *DeepPricing* model. The main difference among the valuation models are the generation models of the underlying stock returns. Daily model prices are compared against daily convertible bond market prices to determine whether there is fair pricing, overpricing or underpricing. Then, the results are pooled to determine the average mispricing for the sample using the mean absolute percentage error (MAPE) defined in Eq. 43:

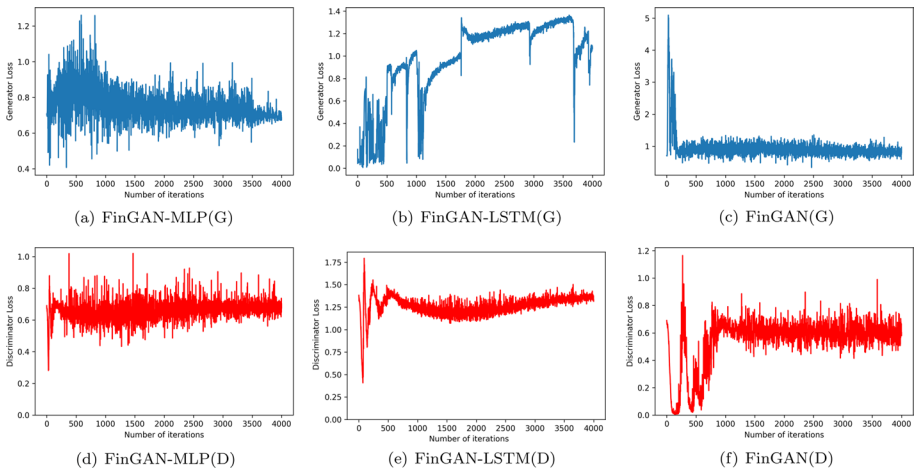

Fig. 5 The loss of FinGAN-MLP, FinGAN-LSTM, *FinGAN* generator (blue) and discriminator (red) in training are presented respectively. The sample period is from November 16, 2006 through June 30, 2021 and includes 3556 observations

$$\text{MAPE} = \frac{1}{N}\sum_{i=1}^{N}\left|\frac{V_i^{\text{Model}} - V_i^{\text{Mkt}}}{V_i^{\text{Mkt}}}\right| \tag{43}$$

where N denote the number of convertible bonds in the daily sample, V_i^{Mkt} is the closed prices of convertible bonds; and V_i^{Model} is the model determined prices for the given model.

Moreover, to measure the extent to which one model is better or worse than another, we compute pricing differences between two models. Let $\Delta\text{MAPE}_{i|j}$ denote the pricing difference of a model i over a model j. $\Delta\text{MAPE}_{i|j}$is defined in Eq. 44:

$$\Delta\text{MAPE}_{i|j} = 100 \times \ln(\text{MAPE}_i/\text{MAPE}_j) \tag{44}$$

where MAPE_i and MAPE_j denote the MAPE implied by models i and j, respectively. A negative (positive) value of $\Delta\text{MAPE}_{i|j}$ means that model i yields lower (higher) pricing errors than model j, implying that the pricing performance of the former is better (worse) than that of the latter by a percentage of that value.

Besides, the mean absolute error (MAE) defined in Eq. 45 and $\Delta\text{MAE}_{i|j}$ defined in Eq. 46 are used for robustness test.

$$\text{MAE} = \frac{1}{N}\sum_{i=1}^{N}\left|V_i^{\text{Model}} - V_i^{Mkt}\right| \tag{45}$$

$$\Delta\text{MAE}_{i|j} = 100 \times \ln(\text{MAE}_i/\text{MAE}_j) \tag{46}$$

Tables 4 and 5 detail MAPE and MAE pricing performance and improvements across different models respectively. The main results for all convertible bonds are offered in

the first line, moreover, the convertible bonds are respectively broken down by equity component levels, market states and moneyness levels in lines 2-5, lines 6-8 and lines 9-11.

Several important conclusions can be drawn from the MAPE performance metrics[8][9]. First, for all convertible bonds in the sample, the *DeepPricing* model has a MAPE of 0.0721. Based on $\Delta\text{MAE}_{i|\text{DeepPricing}}$ metrics, the *DeepPricing* model has a better pricing performance than both model-driven models, i.e. BS, CEV (β=1), GARCH (1,1) and data-driven models, i.e. FinGAN-MLP, FinGAN-LSTM. Secondly, we have broken down convertible bonds' pricing error according to their equity component levels and market states to investigate the ability of the models to fit the structure of the convertible bonds market. Generally speaking, the equity-liked convertible bonds are more likely to be mispriced for all models, as their underlying stock return processes are more volatile and difficult to capture stylized facts. Compared with BS, CEV (β=1), GARCH (1,1), FinGAN-MLP and FinGAN-LSTM models, *DeepPricing* model much better improves the pricing of equity-liked convertible bonds by 26.51%, 23.90%, 17.71%, 12.15%, and 6.86%; and for bull market by 33.97%, 29.33%, 20.51%, 15.83%, and 6.88%. But for lower underlying stock volatility conditions, such as bond-liked convertible bonds or direction-less market, the results are only by 19.14%, 14.24%, 9.56%, 8.37%, and 4.73%; and 14.56%, 13.45%, 8.42%, 4.92%, and 2.04%. The results give evidence that the better fitting performance of our model stems from the improved modeling of the volatility stylized facts of the underlying stock return process. Lastly, we have broken down convertible bonds pricing error according to moneyness levels[10]. Compared with other baseline models, the *DeepPricing* model better improves the pricing of out-of-the-money convertible bonds by 16.99%, 12.82%, 10.50%, 7.54%, and 4.50%, the evidence indicates that the *DeepPricing* model is more flexible to capture the high-dimensional features of the stock return process, outperforming other models in fitting the convertible bond market implied volatility smirk, especially for out-of-the-money convertible bonds. As the main difference between the *DeepPricing* model and other baseline models is the generation methods of the underlying stock return process, i.e. the *FinGAN* model reproduces more accurately stock return series than other generation models, the results also demonstrate the simulation of the dynamic process of the underlying stock return has a better effect on the efficiency of convertible bond pricing, which is consistent with the empirical conclusion of Batten et al. (2018) in USA convertible bond market.

Analysis of mispricing

As the overall pricing efficiency of the Chinese convertible bond market is low, we further analyze the factors affecting the pricing of convertible bonds. The empirical results is provided in Table 6. The dependent variable is the average *DeepPricing* model mispricing degree using the MAPE defined in Eq. 43. The potential influence

[8] The MAE performance metrics for robustness test in Table 5 has also shown the efficiency of the *DeepPricing* model compared to other baseline models.

[9] Notice that all our empirical results are due to the fact that the real daily convertible bonds trading prices are used as a baseline.

[10] Moneyness is defined as the $\xi = S_t/K_t$, where K_t is the conversion price and S_t is the close price of the underlying stock. A convertible bond is said to be out-of-the-money if its $\xi < 0.99$; at the money if $\xi \in [0.99, 1.01]$; in-the-money if $\xi > 1.01$.

Table 4 Pricing performance across different models: MAPE

	BS	CEV($\beta = 1$)	GARCH(1,1)	FinGAN-MLP	FinGAN-LSTM	DeepPricing
Panel A. MAPE						
All	0.0934	0.0924	0.0893	0.0831	0.0797	0.0721
Equity-liked	0.1009	0.0983	0.0924	0.0874	0.0829	0.0774
Balanced	0.0908	0.0827	0.0783	0.0773	0.0746	0.0712
Bond-liked	0.0874	0.0832	0.0794	0.0785	0.0757	0.0722
Bull market	0.1302	0.1243	0.1138	0.1086	0.0993	0.0927
Direction-less market	0.0619	0.0612	0.0582	0.0562	0.0546	0.0535
Bear market	0.0879	0.0874	0.0821	0.0791	0.0769	0.0724
In-the-money	0.0932	0.0926	0.0914	0.0891	0.0862	0.0824
At-the-money	0.0731	0.0713	0.0704	0.0693	0.0681	0.0676
Out-of-the-money	0.0953	0.0914	0.0893	0.0867	0.0841	0.0804
Panel B. $\Delta\text{MAPE}_{i\|\text{CEV}(\beta=1)}$						
All	1.07	0.00	−3.41	−10.61	−14.79	−24.81
Equity-liked	2.61	0.00	−6.19	−11.75	−17.04	−23.90
Balanced	9.31	0.00	−5.47	−6.75	−10.31	−14.97
Bond-liked	4.90	0.00	-4.67	-5.81	-9.47	-14.24
Bull market	4.64	0.00	−8.83	−13.50	−22.46	−29.33
Direction-less market	1.12	0.00	−5.03	−8.52	−11.41	−13.45
Bear market	0.52	0.00	−6.26	−9.98	−12.80	−18.83
In-the-money	0.64	0.00	−1.30	−3.85	−7.16	−11.67
At-the-money	2.48	0.00	−1.27	−2.85	−4.59	−5.33
Out-of-the-money	4.17	0.00	−2.32	−5.28	−8.32	−12.82
Panel C. $\Delta\text{MAPE}_{i\|\text{GARCH(1,1)}}$						
All	4.49	3.41	0.00	−7.20	−11.37	−21.39
Equity-liked	8.80	6.19	0.00	−5.56	−10.85	−17.71
Balanced	14.78	5.47	0.00	−1.29	−4.84	−9.51
Bond-liked	9.58	4.67	0.00	−1.14	−4.77	−9.56
Bull market	13.46	8.83	0.00	−4.68	−13.63	−20.51
Direction-less market	6.14	5.03	0.00	−3.50	−6.39	−8.42
Bear market	6.77	6.26	0.00	−3.72	−6.54	−12.57
In-the-money	1.95	1.30	0.00	−2.55	−5.86	−10.37
At-the-money	3.75	1.27	0.00	−1.57	−3.32	−4.06
Out-of-the-money	6.49	2.32	0.00	−2.95	−6.00	−10.50
Panel D. $\Delta\text{MAPE}_{i\|\text{FinGAN-MLP}}$						
All	11.68	10.61	7.20	0.00	−4.18	−14.20
Equity-liked	14.36	11.75	5.56	0.00	−5.29	−12.15
Balanced	16.10	6.75	1.29	0.00	−3.56	−8.22
Bond-liked	10.74	5.81	1.14	0.00	−3.63	−8.37
Bull market	18.14	13.50	4.68	0.00	−8.95	−15.83
Direction-less market	9.66	8.52	3.50	0.00	−2.89	−4.92
Bear market	10.55	9.98	3.72	0.00	−2.82	−8.85
In-the-money	4.50	3.85	2.55	0.00	−3.31	−7.82
At-the-money	5.34	2.85	1.57	0.00	−1.75	−2.48
Out-of-the-money	9.46	5.28	2.95	0.00	−3.04	−7.54
Panel E. $\Delta\text{MAPE}_{i\|\text{FinGAN-LSTM}}$						
All	15.86	14.79	11.37	4.18	0.00	−10.02
Equity-liked	19.65	17.04	10.85	5.29	0.00	−6.86
Balanced	19.65	10.31	4.84	3.56	0.00	−4.66
Bond-liked	14.37	9.45	4.77	3.63	0.00	−4.73

Table 4 (continued)

	BS	CEV($\beta = 1$)	GARCH(1,1)	FinGAN-MLP	FinGAN-LSTM	DeepPricing
Bull market	27.09	22.46	13.63	8.95	0.00	−6.88
Direction-less market	12.55	11.41	6.39	2.89	0.00	−2.04
Bear market	13.37	12.80	6.54	2.82	0.00	−6.03
In-the-money	7.81	7.16	5.86	3.31	0.00	−4.51
At-the-money	7.09	4.59	3.32	1.75	0.00	−0.74
Out-of-the-money	12.50	8.32	6.00	3.04	0.00	−4.50
Panel F. $\Delta\text{MAPE}_{i\|\text{DeepPricing}}$						
All	25.88	24.81	21.39	14.20	10.02	0.00
Equity-liked	26.51	23.90	17.71	12.15	6.86	0.00
Balanced	24.28	14.97	9.51	8.22	4.66	0.00
Bond-liked	19.14	14.24	9.56	8.37	4.73	0.00
Bull market	33.97	29.33	20.51	15.83	6.88	0.00
Direction-less market	14.56	13.45	8.42	4.92	2.04	0.00
Bear market	19.35	18.83	12.57	8.85	6.03	0.00
In-the-money	12.31	11.67	10.37	7.82	4.51	0.00
At-the-money	7.81	5.33	4.06	2.48	0.74	0.00
Out-of-the-money	16.99	12.82	10.50	7.54	4.50	0.00

Table 4 shows the MAPE performance metrics across the different models. The metric MAPE_i stands for the percentage error of a model *i* as given by Eq. 43. The metric $\Delta\text{MAPE}_{i|j}$ measures the pricing performance difference of a model *i* relative to a model *j*, which is defined by Eq. 44. The debt-liked convertible bonds, the balanced convertible bonds and the equity-liked convertible bonds is determined by the sensitivity of the convertible bond value to its underlying common stock and defined as Δ (Eq. 23) belongingness to the intervals [0, 0.33]; [0.33, 0.66]; and [0.66, 1], respectively. Market states is classified by bull market including subperiod from January 01, 2014 to June 12, 2015 and subperiod from January 01, 2019 to June 30, 2021, bear market including subperiod from January 01, 2010 to December 31, 2013; subperiod from June 15, 2015 to January 29, 2016; subperiod from January 01, 2018 to December 31, 2018 and direction-less market (including subperiod from February 01, 2016 to December 31, 2017. Moneyness is defined as the $\xi = S_t/K_t$, where K_t is the conversion price and S_t is the close price of underlying stock. A convertible bond is said to be out-of-the-money if its $\xi < 0.99$; at the money if $\xi \in [0.99, 1.01]$; in-the-money if $\xi > 1.01$. The sample period is from January 01, 2010 through June 30, 2021 and includes 125,306 observations

factors including time to maturity (*maturity*), credit spread (*credit*), liquidity, underlying stock volatility (*volatility*), the equity component levels, market state, moneyness levels and industry. Notice that we employ two proxies to measure the liquidity of convertible bonds: *amount* (the daily average trading amount) and *turnover* (daily average turnover).

Table 6 reports the regression analysis. A positive coefficient is observed between *amount* and *turnover*, in which convertible bonds with higher liquidity are more likely to be mispriced. This is likely due to there are large number of sentiment-driven investors in Chinese capital market, especially in even less mature convertible bond market (Zhou et al. 2013), Tan et al. 2021). Convertible bonds with higher liquidity are much easier to be hyped by speculative traders, thus, cause market prices deviate from their fundamentals values (Keynes 2018).

Consistently, riskier convertible bonds are more likely to be mispriced as indicated by positive coefficient with *maturity*, *credit* and *volatility*. Convertible bonds with a longer time to maturity, higher rating code (lower quality credit rating), and higher volatility are perceived to be riskier by the market and are expected to be mispriced (Batten et al. 2018).

Table 5 Pricing performance across different models: MAE

	BS	CEV($\beta = 1$)	GARCH(1,1)	FinGAN-MLP	FinGAN-LSTM	DeepPicing
Panel A. MAE						
All	12.0287	11.8763	11.1084	10.8231	10.2431	9.8903
Equity-liked	16.188	15.0215	13.4516	11.4863	10.8942	10.1721
Balanced	9.6481	8.1742	7.6872	7.6196	7.3534	7.0184
Bond-liked	9.325	8.0184	7.4203	7.3255	7.1573	6.9218
Bull market	12.8915	11.7632	10.7654	10.1951	9.7792	9.1293
Direction-less market	6.6288	5.9824	5.7324	5.4552	5.2999	5.1932
Bear market	11.9657	10.9873	9.8935	8.8601	8.6137	8.1097
In-the-money	9.7683	8.2943	7.6729	7.4353	7.1933	6.8762
At-the-money	8.7610	7.4985	7.9832	6.9882	6.5759	6.3291
Out-of-the-money	15.4354	14.8621	14.9824	11.8153	11.4910	10.0295
Panel B. $\Delta\text{MAE}_{i\|\text{CEV}(\beta=1)}$						
All	1.27	0.00	−6.68	−9.29	−14.79	−18.3
Equity-liked	7.48	0.00	−11.04	−26.83	−32.13	−38.98
Balanced	16.58	0.00	−6.14	−7.03	−10.58	−15.24
Bond-liked	15.1	0.00	−7.75	−9.04	−11.36	−14.71
Bull market	9.16	0.00	−8.86	−14.31	−18.47	−25.35
Direction-less market	10.26	0.00	−4.27	−9.23	−12.11	−14.15
Bear market	8.53	0.00	−10.49	−21.52	−24.34	−30.37
In-the-money	16.36	0.00	−7.79	−10.93	−14.24	−18.75
At-the-money	15.56	0.00	6.26	−7.05	−13.13	−16.95
Out-of-the-money	3.79	0.00	0.81	−22.94	−25.73	−39.33
Panel C. $\Delta\text{MAE}_{i\|\text{GARCH}(1,1)}$						
All	7.96	6.68	0.00	−2.60	−8.11	−11.61
Equity-liked	18.52	11.04	0.00	−15.79	−21.09	−27.94
Balanced	22.72	6.14	0.00	−0.88	−4.44	−9.1
Bond-liked	22.85	7.75	0.00	−1.29	−3.61	−6.95
Bull market	18.02	8.86	0.00	−5.44	−9.61	−16.48
Direction-less market	14.53	4.27	0.00	−4.96	−7.84	−9.88
Bear market	19.02	10.49	0.00	−11.03	−13.85	−19.88
In-the-money	24.15	7.79	0.00	−3.15	−6.45	−10.96
At-the-money	9.3	−6.26	0.00	−13.31	−19.39	−23.22
Out-of-the-money	2.98	−0.81	0.00	−23.75	−26.53	−40.13
Panel D. $\Delta\text{MAE}_{i\|\text{FinGAN-MLP}}$						
All	10.56	9.29	2.60	0.00	−5.51	−9.01
Equity-liked	34.31	26.83	15.79	0.00	−5.29	−12.15
Balanced	23.60	7.03	0.88	0.00	−3.56	−8.22
Bond-liked	24.13	9.04	1.29	0.00	−2.32	−5.67
Bull market	23.47	14.31	5.44	0.00	−4.16	−11.04
Direction-less market	19.49	9.23	4.96	0.00	−2.89	−4.92
Bear market	30.05	21.52	11.03	0.00	−2.82	−8.85
In-the-money	27.29	10.93	3.15	0.00	−3.31	−7.82
At-the-money	22.61	7.05	13.31	0.00	−6.08	−9.91
Out-of-the-money	26.73	22.94	23.75	0.00	−2.78	−16.39
Panel E. $\Delta\text{MAE}_{i\|\text{FinGAN-LSTM}}$						
All	16.07	14.79	8.11	5.51	0.00	−3.50
Equity-liked	39.60	32.13	21.09	5.29	0.00	−6.86
Balanced	27.16	10.58	4.44	3.56	0.00	−4.66
Bond-liked	26.46	11.36	3.61	2.32	0.00	−3.35

Table 5 (continued)

	BS	CEV($\beta = 1$)	GARCH(1,1)	FinGAN-MLP	FinGAN-LSTM	DeepPicing
Bull market	27.63	18.47	9.61	4.16	0.00	−6.88
Direction-less market	22.37	12.11	7.84	2.89	0.00	−2.03
Bear market	32.87	24.34	13.85	2.82	0.00	−6.03
In-the−money	30.60	14.24	6.45	3.31	0.00	−4.51
At-the-money	28.69	13.13	19.39	6.08	0.00	−3.83
Out-of-the-money	29.51	25.73	26.53	2.78	0.00	−13.60
Panel F. $\Delta\text{MAE}_{i\|\text{DeepPricing}}$						
All	19.57	18.3	11.61	9.01	3.50	0.00
Equity-liked	46.46	38.98	27.94	12.15	6.86	0.00
Balanced	31.82	15.24	9.1	8.21	4.66	0.00
Bond-liked	29.8	14.71	6.95	5.67	3.35	0.00
Bull market	34.51	25.35	16.48	11.04	6.88	0.00
Direction-less market	24.41	14.15	9.88	4.92	2.03	0.00
Bear market	38.9	30.37	19.88	8.85	6.03	0.00
In-the-money	35.11	18.75	10.96	7.82	4.51	0.00
At-the-money	32.52	16.95	23.22	9.91	3.83	0.00
Out-of-the-money	43.11	39.33	40.13	16.39	13.60	0.00

Table 5 shows the MAE performance metrics across the different models for robustness test. The metric MAE_i stands for the percentage error of a model *i* as given by Eq. 45. The metric $\Delta\text{MAE}_{i|j}$ measures the pricing performance difference of a model *i* relative to a model *j*, which is defined by Eq. 46. The debt-liked convertible bonds, the balanced convertible bonds and the equity-liked convertible bonds is determined by the sensitivity of the convertible bond value to its underlying common stock and defined as Δ (Eq. 23) belongingness to the intervals [0, 0.33]; [0.33, 0.66]; and [0.66, 1], respectively. Market states is classified by bull market including subperiod from January 01, 2014 to June 12, 2015 and subperiod from January 01, 2019 to June 30, 2021, bear market including subperiod from January 01, 2010 to December 31, 2013; subperiod from June 15, 2015 to January 29, 2016; subperiod from January 01, 2018 to December 31, 2018 and direction-less market (including subperiod from February 01, 2016 to December 31, 2017. Moneyness is defined as the $\xi = S_t/K_t$, where K_t is the conversion price and S_t is the close price of underlying stock. A convertible bond is said to be out-of-the-money if its $\xi < 0.99$; at the money if $\xi \in [0.99, 1.01]$; in-the-money if $\xi > 1.01$. The sample period is from January 01, 2010 through June 30, 2021 and includes 125,306 observations

Moreover, the positive sign of *Dequity*, *Dbull* and *Dotm* indicates that equity-liked, trading in bull market and out-of-the-money convertible bonds tend to be more likely to be mispriced. The results is consistent with the empirical results presented in Tables 4 and 5, and this further illustrates the importance of accurately characterizing the volatility and high-dimensional features of the underlying stock return process for the pricing of convertible bonds.

Investment strategies

In this section, we introduce the investment strategies based on *DeepPricing* model. As the regression results in "Analysis of mispricing" section indicate that the Chinese convertible bond market is a weakly efficient market, with the market-wide variations in investor sentiment, the convertible bond prices deviate from their fundamental values temporarily. Therefore, the arbitrageurs will benefit from the arbitrage strategy (*Long-Only Strategy*) - to long underestimated convertible bonds and short overestimated convertible bonds (Keynes 2018). Moreover, as there exits short-sale constraints in Chinese market, we also propose the *Long-Only Strategy* for more practical application. We first introduce the financial concepts used in the process of constructing the strategies, and then the *Long-Short Strategy* and *Long-Only Strategy* are formally proposed. Finally, the

Table 6 Analysis of mispricing

Variables	MAPE	t-value
constant	−0.0037**	(−2.25)
maturity	0.0012***	(3.01)
credit	0.0107***	(28.11)
amount	0.0001***	(26.28)
turnover	0.0025**	(2.05)
volatility	0.1617***	(59.30)
Dequity	0.0128***	(14.28)
Dbalanced	0.0027***	(3.89)
Dbond	−0.0119***	(−20.99)
Dbull	0.0143***	(18.87)
Ddirectionless	−0.0202***	(−11.46)
Dbear	0.0309***	(29.62)
Ditm	−0.0001	(0.59)
Datm	0.0001***	(2.80)
Dotm	0.0034***	(−34.93)
Dfin	−0.0163	(−13.54)

Table 6 reports the results of the regression analysis. The mispricing is measured by MAPE defined in Eq. 43. *maturity* is the time to maturity in years, the numerical values for credit ratings are: $AAA = 1$, $AA+ = 2$, $AA = 3$, $AA- = 4$, $A+ = 5$, $A = 6$, *amount* is the daily average trading amount and *turnover* is the daily average turnover. *volatility*) is the volatility of underlying stock return. *Dequity* is a dummy variable that equals one for an equity-liked convertible bond and zero otherwise. *Dbalanced* is a dummy variable that equals one for a balanced convertible bond and zero otherwise. *Dbond* is a dummy variable that equals one for an bond-liked convertible bond and zero otherwise. *Dbull* is a dummy variable that equals one if the trade is executed in bull market and zero otherwise. *Dbear* is a dummy variable that equals one if the trade is executed in bear market and zero otherwise. *Ddirectionless* is a dummy variable that equals one if the trade is executed in direction-less market and zero otherwise. *Ditm* is a dummy variable that equals one for a in-the-money convertible bond and zero otherwise. *Datm* is a dummy variable that equals one for a at-the-money convertible bond and zero otherwise. *Dotm* is a dummy variable that equals one for an out-of-the-money convertible bond and zero otherwise. *Dfin* is a dummy variable that equals one if the issuer is a financial firm and zero otherwise. ***, ** and * denote significance at 1%, 5%, and 10%, respectively. The sample period is from January 01, 2010 through June 30, 2021 and includes 125,306 observations

evaluation measures have been presented and we show the performance of the strategies in Chinese convertible bond market.

Financial concepts

Following Wang et al. (2019), we introduce some basic financial concepts before proposing investment strategies.

Definition 5 *(Holding period)* A holding period is a minimum time unit to invest a convertible bond. In this work, we divide the time axis as sequential holding periods with fixed length - one day. We call the starting time of the t-th holding period as the time t.

Definition 6 *(Long (Short) position)* The long (short) position is the trading operation that buys (sells) a convertible bond at time t_1 first and then sells (buys) it at t_2. The profit of a long position during the period from t_1 to t_2 for convertible bond i is $v_i(p_{t_2}^{(i)} - p_{t_1}^{(i)})$, while the profit of a short position is $v_i(p_{t_1}^{(i)} - p_{t_2}^{(i)})$, where v_i is the buying (selling) volume of convertible bond i and $p^{(i)}$ is the price of convertible bond i at time t.

Definition 7 *(Investment portfolio)* Given a convertible bond pool with I convertible bonds, a portfolio is defined as a vector $\boldsymbol{c} = (c^{(1)}, ..., c^{(i)}, ..., c^{(I)})^\top$, where $c^{(i)}$ is the proportion of the investment on convertible bond i, with $\sum_{i=1}^{I} c^{(i)} = 1$.

Definition 8 *(Zero-investment portfolio)* A zero-investment portfolio is a collection of convertible bonds portfolios that has a net total investment of zero when the portfolios are assembled. Assume we have a collection of convertible bonds portfolios $\{\boldsymbol{c}^{(1)}, ..., \boldsymbol{c}^{(j)}, ..., \boldsymbol{c}^{(J)}\}$. The investment on portfolio $\boldsymbol{c}^{(j)}$ is $M^{(j)}$, with $M^{(j)} \geq 0$ when taking a long position on and $M^{(j)} \leq 0$ when taking a short position. Then, for a zero-investment portfolio containing J portfolios, the total investment $\sum_{j=1}^{J} M^{(j)} = 0$.

Investment strategies

Long-short strategy

We execute *long-short strategy* as a zero-investment portfolio consisting of two portfolios: a long portfolio for underestimated convertible bonds and a short portfolio for overestimated convertible bonds. Given a sequential investment with T periods, we denote the short portfolio for the t-th period as $\boldsymbol{c}_t^-$ and the long portfolio as $\boldsymbol{c}_t^+, t = 1, ..., T$.

At time t, we first rank the convertible bonds in ascending order in accordance with the mispricing for the sample using the percentage error (PE) based on the *DeepPricing* model price defined in Eq. 47 and partition them into deciles.

$$\mathrm{PE}_{it} = \frac{V_{it}^{\mathrm{Model}} - V_{it}^{\mathrm{Mkt}}}{V_{it}^{\mathrm{Mkt}}} \tag{47}$$

where V_{it}^{Mkt} is the closed prices of convertible bond i at time t, and V_{it}^{Model} is the prices determined by *DeepPricing* model. Notice that $\mathrm{PE}_{it} > 0$ means the convertible bond i is underestimated at time t, while $\mathrm{PE}_{it} < 0$ means the convertible bond i is overestimated at time t.

Then, given a budget constraint $\bar{M}$, we short the convertible bonds ranked in bottom decile in according to the equal or value weighted investment proportion in $\boldsymbol{c}_t^-$ from brokers. The volume of convertible bond i that we can short is

$$v_t^{-(i)} = \bar{M} \cdot c_t^{-(i)} / p_t^{(i)} \tag{48}$$

where $c_t^{-(i)}$ is the proportion of convertible bond i in $\boldsymbol{c}_t^-$. After that, we use $\bar{M}$ to long the convertible bonds ranked in top decile in according to the equal or value weighted investment proportion in $\boldsymbol{c}_t^+$. The volume of convertible bond i that we can long at time t is

$$v_t^{+(i)} = \bar{M} \cdot c_t^{+(i)} / p_t^{(i)} \tag{49}$$

The money $\bar{M}$ we used to long stocks is the proceeds of short selling, so the net investment on the portfolio $\{\boldsymbol{c}_t^+, \boldsymbol{c}_t^-\}$ is zero.

Finally, at the end of the t-th holding period, we sell convertible bonds in the long portfolio. The money we can get is the proceeds of selling convertible bonds using new prices at $t + 1$ for all convertible bonds, i.e.,

$$M_t^+ = \sum_{i=1}^{I} v_t^{+(i)} p_{t+1}^{(i)} = \sum_{i=1}^{I} \bar{M} \cdot c_t^{+(i)} \frac{p_{t+1}^{(i)}}{p_t^{(i)}} \tag{50}$$

Also, we buy the convertible bonds in the short portfolio back and return them to the broker. The money we spend on buying the short convertible bonds is

$$M_t^- = \sum_{i=1}^{I'} v_t^{+(i)} p_{t+1}^{(i)} = \sum_{i=1}^{I'} \bar{M} \cdot c_t^{-(i)} \frac{p_{t+1}^{(i)}}{p_t^{(i)}} \tag{51}$$

The ensemble profit earned by the long and short portfolios is $M_t = M_t^+ - M_t^-$. Let $z_t^{(i)} = p_{t+1}^{(i)}/p_t^{(i)}$ denote the price rising rate of convertible bonds i in the t-th holding period. Then, the rate of return of the ensemble portfolio is calculated as

$$\mathrm{R}_t = \frac{M_t}{\bar{M}} = \sum_{i=1}^{I} c_t^{+(i)} z_t^{(i)} - \sum_{i=1}^{I'} c_t^{-(i)} z_t^{(i)} \tag{52}$$

Long-only strategy

We execute *long-only strategy* at a given budget constraint $\bar{M}$ and long underestimated convertible bonds. Given a sequential investment with T periods, the long portfolio is donated as $\boldsymbol{c}_t^+, t = 1, ..., T$.

At time t, we first rank the convertible bonds in ascending order in accordance with the mispricing for the sample using the percentage error (PE) based on the *DeepPricing* model price defined in Eq. 47 and partition them into deciles.

Then, we only long the convertible bonds ranked in top decile in according to the equal or value-weighted investment proportion in $\boldsymbol{c}_t^+$s. The volume of convertible bond i that we can long at time t is

$$v_t^{+(i)} = \bar{M} \cdot c_t^{+(i)} / p_t^{(i)} \tag{53}$$

At the end of the t-th holding period, we sell convertible bonds in the long portfolio. The money we can get is the proceeds of selling convertible bonds using new prices at $t+1$ for all convertible bonds, i.e.,

$$M_t^+ = \sum_{i=1}^{I} v_t^{+(i)} p_{t+1}^{(i)} = \sum_{i=1}^{I} \bar{M} \cdot c_t^{+(i)} \frac{p_{t+1}^{(i)}}{p_t^{(i)}} \tag{54}$$

Let $z_t^{(i)} = p_{t+1}^{(i)}/p_t^{(i)}$ denote the price rising rate of convertible bonds i in the t-th holding period. Then, the rate of return is calculated as

$$\mathrm{R}_t = \frac{M_t^+}{\bar{M}} = \sum_{i=1}^{I} c_t^{+(i)} z_t^{(i)} \tag{55}$$

Evaluation measures

We select several important evaluation metrics to evaluate the model performance on a standard back-rest platform, including profitability - annualized return, risk - annualized volatility, the maximum drawdown and downside deviation, and performance ratios - Sharpe Ratio, Sortino Ratio and Calmar ratio.

Annualized return (AR) annualized return is an annualized average of return rate. It is defined as $\mathrm{AR}_T = \mathrm{A}_T \times \mathrm{N}_Y$, where N_Y is the number of holding periods in a year.

Annualized volatility (AVOL) annualized volatility is an annualized average of volatility. It is defined as $\mathrm{AVOL}_T = \mathrm{V}_T \times \sqrt{\mathrm{N}_Y}$ and is used to measure the average risk of a strategy during an unit time period.

Max drawdown (MDD) max drawdown is the maximum loss from a peak to a trough of a portfolio, before a new peak is attained. It is the other way to measure the investment risk. The formalized definition of MDD is

$$\mathrm{MDD}_T = \max_{\tau \in [1,T]} \left(\max_{t \in [1,\tau]} \left(\frac{\mathrm{AR}_t - \mathrm{AR}_\tau}{\mathrm{AR}_t} \right) \right) \tag{56}$$

Downside deviation (DD) downside deviation ratio measures the downside risk of a strategy as the average of returns when it falls below a minimum acceptable return (MAR). The formalized definition of DD is given as

$$\mathrm{DD}_T = \sqrt{\mathbb{E}[\min(\mathrm{R}_t, \mathrm{MAR})]^2} \tag{57}$$

Annualized sharpe ratio (ASR) Annualized sharpe ratio is a risk-adjusted profit measure based on AR and AVOL.The formalized definition of ASR is $\mathrm{ASR}_T = \mathrm{AR}_T / \mathrm{AVOL}_T$.

Sortino ratio (STR): Sortino ratio is a risk-adjusted profit measure based on AR and DD. The formalized definition of STR is $\mathrm{STR}_T = \mathrm{AR}_T / \mathrm{DD}_T$.

Calmar ratio (CR): Calmar ratio is a risk-adjusted profit measure based on AR and MDD. The formalized definition of CR is $\mathrm{CR}_T = \mathrm{AR}_T / \mathrm{MDD}_T$.

Strategy performance

Figure 6 are the equally-weighted and value-weighted cumulative returns of *Long-Short Strategy* and *long-only strategy*, respectively. In general, during the sample period from January 01, 2018 to June 30, 2021, *Long-Short Strategy* earns annualized return with 41.16% and 42.52% annualized return for equally-weighted portfolio and value-weighted portfolio, respectively. And *long-only strategy* earns annualized return with 31.06% and 37.09% annualized return for equally-weighted portfolio and value-weighted portfolio, respectively. Moreover, the performances evaluated by other measures are listed in Table 7[11].

Conclusion

In this paper, we propose *DeepPricing*, a *FinGAN* based model for pricing convertible bonds. Extending traditional model-driven stock return generators, the method is more flexible and accurate than the baseline methods to capture dynamics of the underlying

[11] Notice that strategy returns are computed in the absence of transaction costs.

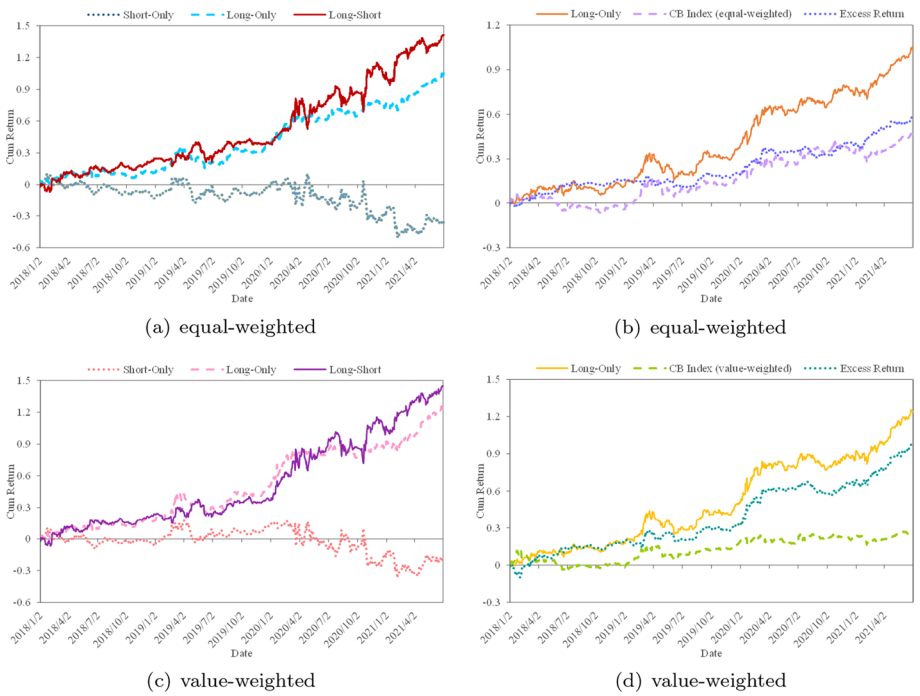

Fig. 6 The cumulative return in Chinese convertible bond market based on *DeepPricing* model, the sample period is from January 01, 2018 through June 30, 2021

stock return process by adopting a novel financial time-series generative adversarial networks, as it is able to reproduce risk-neutral stock return process that retains the major stylized facts such as the linear unpredictability, the fat-tailed distributions, the volatility clustering, the leverage effects, the coarse-fine volatility correlation, and the gain/loss asymmetry.

We implement the *DeepPricing* model and conduct an extensive empirical pricing study for the Chinese convertible bond market, covering daily prices from January 01, 2010 to June 30, 2021. Several important conclusions can be drawn. First, the *DeepPricing* model has a much better convertible bonds pricing performance than the traditional model-based generators such as BS, CEV, GARCH and data-driven generators such as FinGAN-MLP and FinGAN-LSTM. Second, we find that due to the higher reproducibility of stylized facts, the *DeepPricing* model substantially improves the pricing of equity-liked convertible bonds, the convertible bonds trading in the bull market and out-of-the-money convertible bonds. The results indicate that the *DeepPricing* model is more flexible to capture the volatility and high-dimensional features of the underlying stock return process, outperforming other models in fitting higher volatility convertible bonds and the overall market implied volatility smirk. Third, we analyze the factors affecting the pricing of convertible bonds. Empirical results show that convertible bonds which are higher-liquidity, riskier (longer time to maturity, lower quality credit rating, higher volatility), equity-liked, trading in the bull market and out-of-the-money tend to be more likely to be mispriced. The results are consistent with the convertible bond pricing performance, and further illustrate the importance of accurately characterizing the volatility and high-dimensional features for the pricing of convertible bonds. Finally,

Table 7 Strategy performance in Chinese convertible bond market based on *DeepPricing* model

	AR	AVOL	MDD	DD	ASR	STR	CR
Equally-weighted							
Panel A.1. Long-short strategy							
Long-short	0.4116	0.3260	0.2178	0.1985	1.2626	2.0737	1.8901
Long-only	0.3106	0.1653	0.1034	0.1094	1.8793	2.8389	3.0049
Short-only	−0.1009	0.3629	0.2541	02787	−0.2782	−0.3622	−0.3973
Panel A.2. Long-only strategy							
Long-only	0.3106	0.1653	0.1034	0.1094	1.8793	2.8389	3.0049
Convertible bonds Index (equally-weighted)	0.1394	0.1324	0.0739	0.0929	1.0533	1.5004	1.8873
Excess return	0.1712	0.0987	0.0566	0.0598	1.7353	2.8615	3.0249
Value-weighted							
Panel B.1. Long-short strategy							
Long-short	0.4252	0.3300	0.2409	0.2054	1.2884	2.0701	1.7650
Long-only	0.3709	0.2050	0.1562	0.1284	1.8089	2.8879	2.3737
Short-only	−0.0543	0.3395	0.2389	0.2569	−0.1600	−0.2115	−0.2274
Panel B.2. Long-only strategy							
Long-only	0.3709	0.2050	0.1562	0.1284	1.8089	2.8879	2.3737
Convertible bonds Index (value-weighted)	0.0789	0.1116	0.0828	0.0774	0.7064	1.0194	0.9521
Excess return	0.2920	0.1509	0.0998	0.0854	1.9356	3.4185	2.9252

Table 7 reports the evaluation metrics of *Long-short strategy* and *Long-only strategy*, respectively. AR stands for annualized return, AVOL stands for annualized volatility, MDD stands for max drawdown, DD stands for downside deviation, ASR stands for annualized Sharpe ratio, STR stands for sortino ratio, CR stands for calmar ratio. The sample period is from January 01, 2018 through June 30, 2021

the investment strategies based on the *DeepPricing* model are proposed. Both *long-short strategy* and *long-only strategy* earn a significant annualized return with 41.16% and 31.06% for equally-weighted portfolio and 42.52% and 37.09% for the value-weighted portfolio during the sample period, respectively.

This paper provides a new attempt to apply the GAN-based method for the pricing of convertible bonds. For future research, it can be applied for the pricing of other complex path-dependent derivatives.

Appendix

The implement details of *FinGAN*

We use TensorFlow to implement *FinGAN*. For all of the components (encoder, decoder, generator, and discriminator networks), we used TCNs with skip connections. Inside the TCN architecture, the block module is composed of temporal blocks each containing two dilated causal convolutions and two PReLUs as activation functions. The TCN architecture is illustrated in Table 8. Table 9 shows the input, hidden and output dimensions of the models. Note that for all models, the hidden dimension was set to 80, the kernel size of each temporal block, except the first block, was 2, and the receptive field size of each TCN is 127.

Table 8 The TCN architecture of the models

Module name	Arguments
Temporal block 1	(N_I,N_H,N_H,1,1)
Temporal block 2	(N_H,N_H,N_H,2,1)
Temporal block 3	(N_H,N_H,N_H,2,2)
Temporal block 4	(N_H,N_H,N_H,2,4)
Temporal block 5	(N_H,N_H,N_H,2,8)
Temporal block 6	(N_H,N_H,N_H,2,16)
Temporal block 7	(N_H,N_H,N_H,2,32)
1×1 Convolution	(N_H,N_O,1,1)

Table 8 reports the specific arguments of the TCN architecture. A TCN is composed of multiple temporal block modules with arguments (N_I, N_H, N_O, K, D) and an 1×1convolution layer, where N_I stands for the input dimension,N_H stands for the hidden dimension,N_O stands for the output dimension data,K stands for the kernel size, and D stands for the dilation. The temporal block modules used in TCN mainly refer to Bai et al. (2018), and the specific module construction details are in http://github.com/locuslab/TCN

Table 9 Configuration of the encoder (Enc), decoder (Dec), generator (G) and discriminator (D) of the *FinGAN* models

Models	TCN-Enc	TCN-Dec	TCN-G	TCN-D
N_I	1	1	3	1
N_H	80	80	80	80
N_O	2	1	2	1

Table 9 reports the specific parameters of the *FinGAN* model, where N_I stands for the dimension of input layer, N_H stands for the dimension of the hidden layer, and N_O stands for the dimension of the output layer

Acknowledgements
We are grateful to helpful comments from Gang Kou (the editor) and four anonymous referee. We also benefitted from the discussions with Yeqing Zhang.

Author contributions
All authors collaborated closely on the subject. In particular, XYT: Conceptualization, Methodology, Algorithm, Writing-Original Draft. ZLZ: Conceptualization, Methodology, Supervision. XJZ: Conceptualization, Reviewing, Supervision. SYW: Conceptualization, Methodology, Algorithm, Visualization, Editing. All authors read and approved the final manuscript. .

Funding
This work has been supported by the Postdoctoral Science Foundation of China (Project No.2021M700055). Xiaoyu Tan has been supported by Special Fund for Postdoctoral Funding for Shanghai and Science and Technology Development in Shanghai Pudong New Area.

Availability of data and materials
All data were collected from Wind Database and Bloomberg Database. The Wind Database can be accessed at https://www.wind.com.cn, and the Bloomberg can be accessed at https://www.bloomberg.com/professional/.

Declarations

Competing interests
The authors declare that they have no competing interests.

Author details
[1]Guanghua School of Management, Peking University, Beijing 100871, China. [2]Harvest Fund Management, Beijing 100020, China. [3]Department of Mathematics, Zhejiang University, Hangzhou 310027, China.

Received: 2 September 2021 Accepted: 22 May 2022
Published online: 06 June 2022

References
Ammann M, Kind A, Wilde C (2008) Simulation-based pricing of convertible bonds. J Empir Finance 15(2):310–331

Ayache E, Forsyth PA, Vetzal KR (2003) Valuation of convertible bonds with credit risk. J Deriv 11(1):9–29
Barone-Adesi G, Bermúdez A, Hatgioannides J (2003) Two-factor convertible bonds valuation using the method of characteristics/finite elements. J Econ Dynamics Control 27(10):1801–1831
Batten JA, Khaw KLH, Young MR (2018) Pricing convertible bonds. J Bank Finance 92:216–236
Black F, Scholes M (1973) The pricing of options and corporate liabilities. J Polit Econ 81(3):637–654
Bollerslev T (1986) Generalized autoregressive conditional heteroskedasticity. J Econom 31(3):307–327
Bouchaud J-P, Matacz A, Potters M (2001) Leverage effect in financial markets: the retarded volatility model. Phys Rev Lett 87(22):228701
Brennan MJ, Schwartz ES (1977) Convertible bonds: valuation and optimal strategies for call and conversion. J Finance 32(5):1699–1715
Brown SJ, Grundy BD, Lewis CM, Verwijmeren P (2012) Convertibles and hedge funds as distributors of equity exposure. Rev Financ Stud 25(10):3077–3112
Buchan MJ (1997) Convertible bond pricing: theory and evidence. Harvard University, Cambridge
Burlacu R (2000) New evidence on the pecking order hypothesis: the case of French convertible bonds. J Multinatl Financ Manag 10(3–4):439–459
Chakraborti A, Toke IM, Patriarca M, Abergel F (2011) Econophysics review: I. Empirical facts. Quant Finance 11(7):991–1012
Chambers DR, Lu Q (2007) A tree model for pricing convertible bonds with equity, interest rate, and default risk. J Deriv 14(4):25–46
Christie AA (1982) The stochastic behavior of common stock variances: value, leverage and interest rate effects. J Financ Econ 10(4):407–432
Cont R (2001) Empirical properties of asset returns: stylized facts and statistical issues. Quant Finance 1(2):223
Cont R (2007) Volatility clustering in financial markets: empirical facts and agent-based models. In: Teyssiere G, Kirman AP (eds) Long memory in economics. Springer, Berlin, pp 289–309
Dogariu M, Ştefan L-D, Boteanu BA, Lamba C, Kim B, Ionescu B (2022) Generation of realistic synthetic financial time-series. ACM Trans Multimed Comput Commun Appl (TOMM) 18(4):1–27
Duan JC (1995) The GARCH option pricing model. Math Finance 5(1):13–32
Fan C, Luo X, Wu Q (2017) Stochastic volatility vs. jump diffusions: evidence from the Chinese convertible bond market. Int Rev Econ Finance 49:1–16
Gavrishchaka VV, Ganguli SB (2003) Volatility forecasting from multiscale and high-dimensional market data. Neurocomputing 55(1–2):285–305
Goodfellow I, Bengio Y, Courville A (2016) Deep learning. MIT Press, UK
Gupta A, Zou J (2019) Feedback GAN for DNA optimizes protein functions. Nat Mach Intell 1(2):105–111
Hung MW, Wang JY (2002) Pricing convertible bonds subject to default risk. J Deriv 10(2):75–87
Ingersoll JE Jr (1977) A contingent-claims valuation of convertible securities. J Financ Econ 4(3):289–321
Jensen MH, Johansen A, Simonsen I (2003) Inverse statistics in economics: the gain-loss asymmetry. Phys A Stat Mech Appl 324(1–2):338–343
Keynes JM (2018) The general theory of employment, interest, and money, 2nd edn. Springer, UK
Koshiyama A, Firoozye N, Treleaven P (2021) Generative adversarial networks for financial trading strategies fine-tuning and combination. Quant Finance 21(5):797–813
Lewis CM (1991) Convertible debt: valuation and conversion in complex capital structures. J Bank Finance 15(3):665–682
Lin S, Zhu S-P (2020) Numerically pricing convertible bonds under stochastic volatility or stochastic interest rate with an adi-based predictor–corrector scheme. Comput Math Appl 79(5):1393–1419
Liu Y, Gopikrishnan P, Stanley HE et al (1999) Statistical properties of the volatility of price fluctuations. Phys Rev E 60(2):1390
Longstaff FA, Schwartz ES (2001) Valuing American options by simulation: a simple least-squares approach. Rev Financ Stud 14(1):113–147
Ma C, Xu W, Yuan G (2020) Valuation model for Chinese convertible bonds with soft call/put provision under the hybrid willow tree. Quant Finance 20(12):2037–2053
Malmsten H, Teräsvirta T (2010) Stylized facts of financial time series and three popular models of volatility. Eur J Pure Appl Math 3(3):443–477
Merton RC (1973) Theory of rational option pricing. Bell J Econ Manag Sci 4:141–183
McConnell JJ, Schwartz ES (1986) LYON taming. J Finance 41(3):561–576
Merton RC (1974) On the pricing of corporate debt: the risk structure of interest rates. J Finance 29(2):449–470
Müller UA, Dacorogna MM, Davé RD, Olsen RB, Pictet OV, Von Weizsäcker JE (1997) Volatilities of different time resolutions-analyzing the dynamics of market components. J Empir Finance 4(2–3):213–239
Nyborg KG (1996) The use and pricing of convertible bonds. Appl Math Finance 3(3):167–190
Qiu T, Zheng B, Ren F, Trimper S (2006) Return-volatility correlation in financial dynamics. Phys Rev E 73(6):065103
Shreve SE (2004) Stochastic calculus for finance II: continuous-time models. Springer, New York
Takahashi A, Kobayashi T, Nakagawa N (2001) Pricing convertible bonds with default risk. J Fixed Income 11(3):20–29
Takahashi S, Chen Y, Tanaka-Ishii K (2019) Modeling financial time-series with generative adversarial networks. Phys A Stat Mech Appl 527:121261
Tan X, Zhang Z, Zhao X, Wang C (2021) Investor sentiment and limits of arbitrage: evidence from Chinese stock market. Int Rev Econ Finance 75:577–595
Tsiveriotis K, Fernandes C (1998) Valuing convertible bonds with credit risk. J Fixed Income 8(2):95
Wiese M, Knobloch R, Korn R, Kretschmer P (2020) Quant GANs: deep generation of financial time series. Quant Finance 20(9):1419–1440
Yagi K, Sawaki K (2010) The valuation of callable-puttable reverse convertible bonds. Asia-Pac J Oper Res 27(02):189–209
Zhang K, Zhong G, Dong J, Wang S, Wang Y (2019) Stock market prediction based on generative adversarial network. Proced Comput Sci 147:400–406

Zhou M, Huang W, Dong Z, Fang X (2013) Can the pricing efficiency of Chinese convertible bonds be improved? Analysis from the perspective of the cost of arbitrage. China Econ Q 4:1278–1298
Zhu S-P (2006) A closed-form analytical solution for the valuation of convertible bonds with constant dividend yield. ANZIAM J 47(4):477–494
Zhu S-P, Lin S, Lu X (2018) Pricing puttable convertible bonds with integral equation approaches. Comput Math Appl 75(8):2757–2781
Bai S, Kolter JZ, Koltun V (2018) An empirical evaluation of generic convolutional and recurrent networks for sequence modeling. arXiv preprint arXiv:1803.01271
Chung J, Gulcehre C, Cho K, Bengio Y (2014) Empirical evaluation of gated recurrent neural networks on sequence modeling. arXiv preprint arXiv:1412.3555
Cox JC (1996) The constant elasticity of variance option pricing model. 47-98, J Portf Manag 15:79–98
Donahue C, McAuley J, Puckette M (2018) Synthesizing audio with generative adversarial networks. arXiv preprint arXiv:1802.04208
Esteban C, Hyland SL, Rätsch, G (2017) Real-valued (medical) time series generation with recurrent conditional GANs. arXiv preprint arXiv:1706.02633
Farimani AB, Gomes J, Pande VS (2017) Deep learning the physics of transport phenomena. arXiv preprint arXiv:1709.02432
Gan C, Huang D, Chen P, Tenenbaum JB, Torralba A (2020) Foley music: learning to generate music from videos. In: European conference on computer vision. Springer, Cham, pp 758–775
Garbacea C, Carton S, Yan S, Mei Q (2019) Judge the judges: a large-scale evaluation study of neural language models for online review generation. arXiv preprint arXiv:1901.00398
Goodfellow I, Pouget-Abadie J, Mirza M, Xu B, Warde-Farley D, Ozair S, Courville A, Bengio Y (2014) Generative adversarial nets. Adv Neural Inf Process Syst 27
Hadad N, Wolf L, Shahar M (2018) A two-step disentanglement method. In: Proceedings of the IEEE conference on computer vision and pattern recognition, pp 772–780
Karras T, Aittala M, Laine S, Härkönen E, Hellsten J, Lehtinen J, Aila T (2021) Alias-free generative adversarial networks. Adv Neural Inf Process Syst 34
Killoran N, Lee LJ, Delong A, Duvenaud D, Frey BJ (2017) Generating and designing DNA with deep generative models. arXiv preprint arXiv:1712.06148
Li D, Chen D, Jin B, Shi L, Goh J, Ng S-K (2019) MAD-GAN: multivariate anomaly detection for time series data with generative adversarial networks. In: International conference on artificial neural networks. Springer, Cham, pp 703–716
Pascanu R, Mikolov T, Bengio Y (2013) On the difficulty of training recurrent neural networks. In: International conference on machine learning. PMLR, pp 1310–1318
Radford A, Metz L, Chintala S (2015) Unsupervised representation learning with deep convolutional generative adversarial networks. arXiv preprint arXiv:1511.06434
Salimans T, Goodfellow I, Zaremba W, Cheung V, Radford A, Chen X (2016) Improved techniques for training GANs. Adv Neural Inf Process Syst 29
Sun C, Hong S, Song M, Li H (2020) A review of deep learning methods for irregularly sampled medical time series data. arXiv preprint arXiv:2010.12493
Wang J, Zhang Y, Tang K, Wu J, Xiong Z (2019) Alphastock: a buying-winners-and-selling-losers investment strategy using interpretable deep reinforcement attention networks. InProceedings of the 25th ACM SIGKDD international conference on knowledge discovery & data mining, pp 1900–1908
Yang LC, Chou SY, Yang YH (2017) Midinet: a convolutional generative adversarial network for symbolic-domain music generation. arXiv preprint arXiv:1703.10847
Zhang Y, Gan Z, Carin L (2016) Generating text via adversarial training. In: NIPS workshop on adversarial training, vol 21. Academia. edu, San Francisco, pp 21–32

Publisher's Note